ACOUSTIC MANIPULATION WITH ELASTOMERIC PARABOLIC REFLECTORS AND APPLIED VACUUM

By

SAURABH SANJAY APTE

A thesis submitted to the

School of Graduate Studies

Rutgers, The State University of New Jersey

In partial fulfillment of the requirements

For the degree of

Master of Science

Graduate Program in Mechanical and Aerospace Engineering

Written under the direction of

Aaron D. Mazzeo

And approved by

_____

_____

_____

_____

New Brunswick, New Jersey

January 2018

ABSTRACT OF THE THESIS

ACOUSTIC MANIPULATION WITH ELASTOMERIC PARABOLIC REFLECTORS AND APPLIED VACUUM

By SAURABH SANJAY APTE

Thesis Director:

Aaron D. Mazzeo

This thesis describes a parabolic acoustic reflector with an inflatable reflecting surface, which has tunable gain and directivity. Conventional parabolic reflectors focus and amplify sound waves using metallic or plastic dishes with fixed geometries. This work presents a morphable reflecting surface that deforms into a concave structure to provide polar response and tunable gain considering the deformed geometry of the reflector. The deformable concave structure was a silicone elastomer (Ecoflex 00-10) with a coefficient of reflection approximately 0.9. This reflective coefficient suggests these silicone-based elastomers serve as reflective substrates for advanced morphable devices to manipulate sound. We experimentally determined the Youngs Modulus and the radial displacement achieved during pre-stressing the membrane over the aluminum reflector. For our parabolic reflector, acoustic gain and directionality depended on the level of vacuum applied to the elastomeric membranes, which affected the curvature of the paraboloid. Experiments performed in closed and open environments, along with simulations, demonstrate that the soft reflective surface was capable of transformation

into a set of desired parabolic shapes between an initial planar geometry (neutral position) and configurations with varying curvature. The magnitude of the acoustic power gain obtained for vacuums below -1.7 kPa at frequencies greater than 7 kHz was comparable with gains of commercially available reflectors, and the directional response of the reflector was super hyper cardioid in nature. The maximum gain was also ~17 dB at 8.5 kHz. Simulations coupling mechanical deformation with acoustic shells agreed qualitatively with experimental results. These systems might find future uses for adjustable parabolic microphones, long-range communication devices, and tracking of sound sources.

Acknowledgement

I would like to take this opportunity to especially thank Prof. Aaron Mazzeo, Eric, Ni, Xiyue Zhou, Tongfen Liang for helping me through this project. I am highly grateful to Yanjun Wang for his able guidance and prompt responses to my queries prior to and post graduating from Rutgers. I would also like to thank Jingjin Xie for his sharing his design expertise with me which aided me to design my components. I am thankful to Prof. Mitsonuri Denda, Prof. Jonathan Singer and Prof. Rajiv Malhotra for being on the committee of my thesis defense.

Dedication

I would like to dedicate this thesis to my parents and Prof Aaron Mazzeo who gave me an opportunity to work on such a hands-on and exciting project. The resources I received from the lab and the skill-set I earned while working on my thesis is beyond my imagination.

Table of Contents

List of Illustrations:

List OF Tables

1.Introduction

An acoustic mirror is a device that collects and focuses sound at the fixed focus. Acoustic mirrors have found applications during the world war, to detect an approaching aircraft, by focusing the sound waves emitted by its engine. “Whisper Galleries” have been a popular exhibit in the museum to demonstrate focusing of sound. Such galleries are present at Bristol Science Museum in the UK, the Science Museum of Minnesota. An acoustic mirror is typically a huge structure with an average height of 10-12m.

A parabolic microphone is also a device used for sound amplification by focusing sound energy. They are extremely directional devices. When the dish aimed at a distant sound source, a sensitive microphone placed at the focus point will receive an enhanced signal level due to the acoustic energy arriving over the entire aperture of the dish. Since the dish microphone is effective in enhancing sounds from distant objects, we often use it to obtain the sound from a source placed at a distance.

The acoustical gain of a dish microphone is like that of a dish antenna since the wave physics are essentially the same. The dish area, focal length and the dish diameter are the characteristic dimensions of the dish microphone. The dish area is the area normal to the incident sound waves. The efficiency of the reflector dish typically ranges between 45-55%. [1]:

$$Gain\ (dB)\ = 20 * log_{10}(\eta * (\frac{\pi * D}{\lambda})^2) \quad \textbf{(1)}$$

The focal length of the parabola is:

$$F = \frac{D^2}{16 * H} \quad \textbf{(2)}$$

Where; H is the depth of the parabola[2]. Parabolic collectors and reflectors have an immediate day to day applications which include sporting events, wildlife sound collection, event video graphing, independent filmmakers. The typical materials used for parabolic reflector are plastics, polymers, and fiberglass.

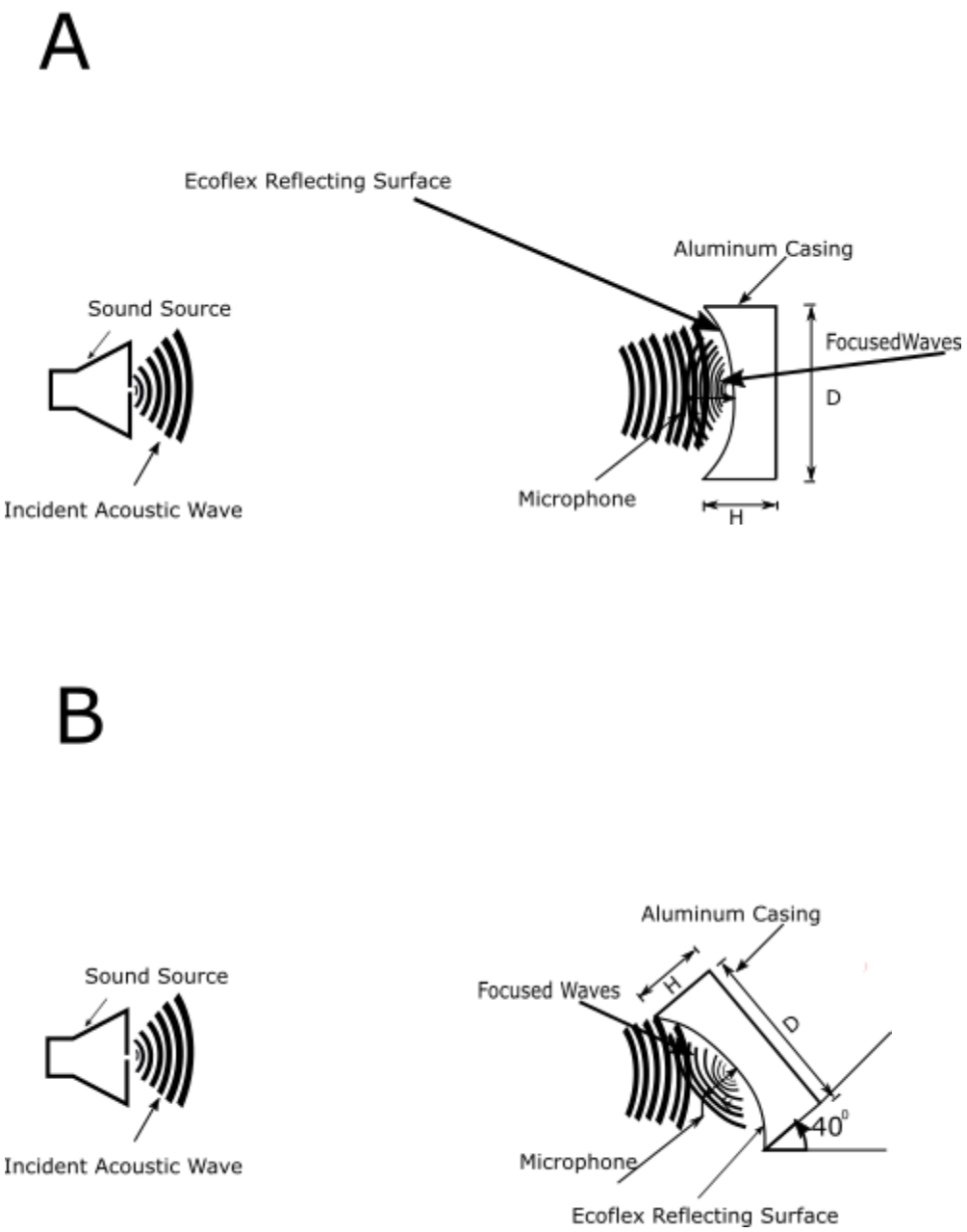

Figure 1: Figure (A) indicates the focusing of acoustic waves originating from a sound source on a microphone placed at the focus. We place the sound source and the reflector axially. Figure (B) indicates the focusing of acoustic waves originating from a sound source on a microphone placed at the focus of the reflector inclined at 40^0.

1.1 Acoustic Parabolic Reflector

Acoustic reflectors mainly consist of convex, concave and blunt surfaces. A convex surface scatters sound, and concave surface focusses sound. Convex reflectors typically find application in building and room acoustics (e.g., Ceiling reflectors) [3]. The applications of sound focusing include wild-life sound focusing, underwater acoustics, sonic lenses, crowd control using" Focused Sound Laser". The parabolic acoustic reflectors have gained popularity and have widespread applications. But the hard-parabolic reflectors have a fixed geometry and hence a fixed focus. By directionality, a microphone can pick up sound from all directions. We monitor directionality using a polar response pattern. Cardioid, bidirectional and omnidirectional are the different categories of microphones that are available commercially[4]. The parabolic reflector antenna is ideal for high gain applications. The antenna gain directly depends upon the diameter of the reflecting surface, operational wavelength, and dish efficiency. The gain of a typical 6-foot dish antenna can be as high as 50 dB.

The antenna gain directly depends upon the diameter of the reflecting surface, operational wavelength, and dish efficiency. The beam width indicates the points where the power falls to half of the maximum, i.e., the -3dB points on a radiation pattern polar diagram[5]. The beam width is determined as follows:

$$Beam\ Width\ \Psi\ = \frac{70 * \lambda}{D} \qquad \textbf{(3)}$$

Where: D is the diameter of the parabola.

Tetsuya Takiguchi[1] , Ryoichi Takashima[2] and Yasuo Ariki[3] in their paper “Evaluation of an Active Microphone with a Parabolic Reflection Board for Monaural Sound-Source-Direction Estimation” made use of parabolic reflection board to detect the sound direction by comparing the difference between the acoustic transfer functions of the target and non-target directions[6].

1.2 Objective

In this thesis, we intend to observe the gain and directionality of a reflector with an elastomeric reflective surface. We made use of a of Ecoflex 00-10 as the reflecting surface. Since Ecoflex being a non-porous material, when arranged like a stretched drum membrane in conjunction with an aluminum reflector, the entire assembly is vacuum tight. Zhixin [2].

We primarily designed an aluminum reflector housing for mounting on a tripod-fixture assembly. We implemented special measures to make the assembly vacuum tight. The vacuum inside the reflector assembly dictates the deformed profile of Ecoflex 00-10. Thus, with variation in the depth, the focus of the parabola changes giving rise to varying amplification of incoming sound waves. Yanjun Wang in his thesis titled "Acoustic manipulation of sound with soft material-based actuators" demonstrates the use of elastomeric actuators to focus incoming sound waves[7] . This thesis builds upon his work by further exploring the two parameters gain and directionality for distinct vacuums applied to the Ecoflex membrane. We performed simulations using COMSOL acoustic shell interaction submodule to confirm the nature of the plots obtained experimentally. We performed acoustic filtering for frequencies in the range 50 Hz to 10,000 Hz. We attempted to demonstrate directionality audio-visually. We obtained the Young's Modulus and Radial displacement of the Ecoflex 00-10 membrane experimentally and by performing simulations using COMSOL Multiphysics.

2. Experimental Design

2.1 Aluminum Reflector assembly

We intend to conduct on-axis acoustic testing of a 9-inch aluminum reflector. The aluminum reflector assembly consists of a hollow aluminum casing and an Ecoflex membrane (0.4-inch-thick and 11-inch diameter) assembled like a pre-stressed drum membrane. The Ecoflex membrane is pre-tensioned by stretching it uniformly. It secured against the wall of the reflector using rubber bands. We used hose clamps to clamps the secured membrane against the walls of the reflector. The grade of Aluminum is 6061. The Aluminum reflector has ¼’’-20 internal threading at its bottom. We screw a steel mount post at its bottom which further aides it's mounting. The reflector has 0.7’’ diameter hole at its back with 1/8’’ NPT (National Pipe Thread) internal threading. We use a 1/8’’ NPT barbed tube steel connector at its back. We implemented a chamfer of 0.1’’ on sharp edges and rims. The reflector has a thickness of 0.5 inches on the front face.

Ecoflex 00-10 is a soft silicone-based rubber with a Shore A Hardness of 00-10. We mixed 300 g of Part A with 300 g of part B in 1:1 ratio by weight. Acrylic molds were laser cut from a 12-inch square acrylic sheet. We used acrylic to mold a uniform membrane with equal properties in all directions. The membrane had a cure time of 10 hours.

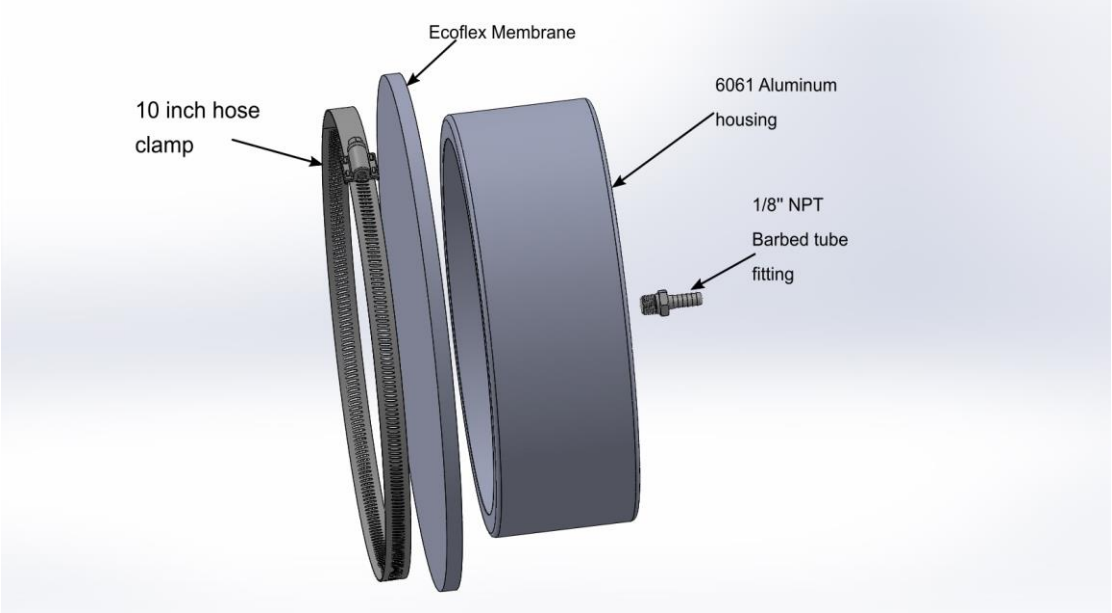

Figure 2: Exploded view of the reflector assembly drafted using SolidWorks 2016.

2.2 Plumbing for measuring Vacuum

As stated earlier, we made the assembly airtight by using a hose clamp. The vacuum forces acting on the membrane keep the deformed membrane in place. We measured the vacuum in the assembly using a Panasonic ADP5 Pressure transducer and a U-tube digital manometer.

The Panasonic ADP5 is a pressure transducer with a built-in circuit and an amplifier. The sensor measures pressure within the range -100 KPa to 100 KPa (Gauge Pressure). The sensor has an accuracy of ± 1.25%. We used a 3-way barbed connector to connect the reflector assembly and the vacuum sensor. The bred board had the sensor plugged into it. The corresponding voltage determined by the analog pin (A0) calibrates the pressure. We used the sealant tapes to keep the assembly airtight.

The AR1890 is a digital manometer to measure differential pressure. We connect one end of the manometer to the assembly and expose the other to the atmosphere.

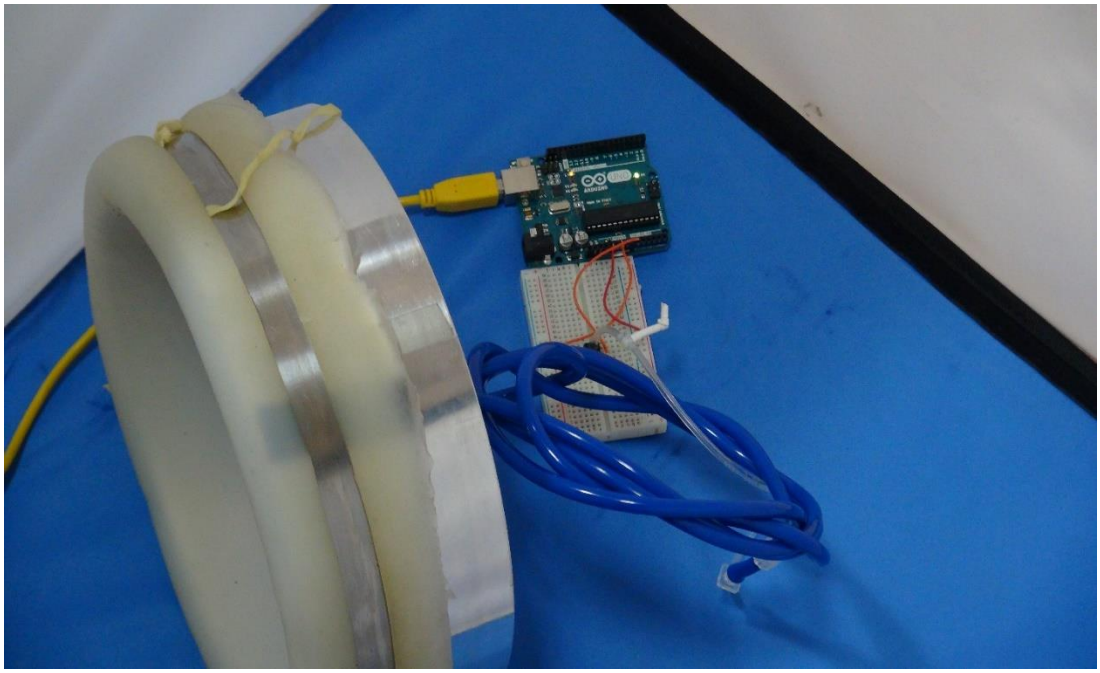

Figure 3: Panasonic ADP5 chip mounted on a bred board to measure vacuum inside the reflector. The “A0” pin of Arduino measures the analog voltage which converts it into pressure.

Figure 4: Digital U-tube manometer to measure vacuum inside the reflector assembly. We keep one end of the manometer exposed to the atmosphere. The manometer indicates differential pressure in (-kPa). The manometer has the options to record and switch between unit systems.

2.3 Determination of Young's Modulus

Ecoflex rubbers are platinum-catalyzed silicones. Part A and Part B solutions were mixed in 1:1 ratio, 70 g each to prepare the Ecoflex strip. The two solutions were de-aired for 10 minutes using a vacuum pump. We de-aired, mixed the two solutions and poured them into a 3D printed mold. The cure time was about 5 hrs. A strip 2.93-inch-long, 0.075-inch-deep and 0.703 inch wide.

The Young's modulus of Ecoflex 00-10 was determined by suspending it as a cantilever and mapping its deflection. The suspension length was 0.8 inches. We took a photograph of the deflected profile[8]:

$$\frac{d^2}{dx^2}\left(E * I * \frac{d^2 y(x)}{dx^2}\right) = Q \qquad \textbf{(4)}$$

Where; y(x) represents the curve of deflection at a given point x. Q is the uniform self-weight.

We suspended the strip at 8 inches from the ground using a stand and photographed the deflected profile of the Ecoflex strip a digital camera with a graph paper in the background. The fixed length was 0.8 inch.

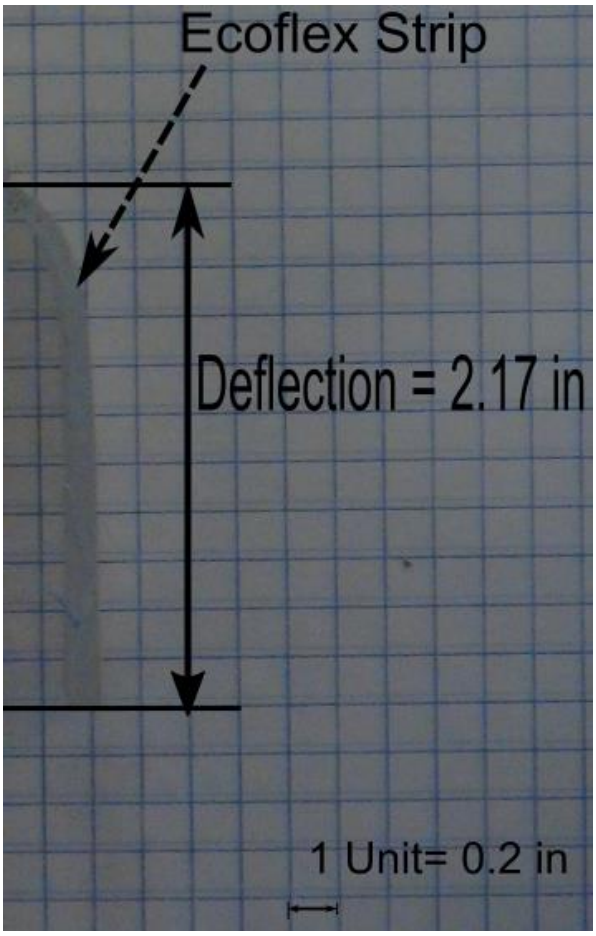

Figure 5: Experimental Setup to physically plot the displaced profile of an Ecoflex strip suspended as a cantilever beam with a suspension length of 0.8 inches.

2.4 Experimental determination of Radial Displacement

The aluminum reflector has a reflecting surface made from Ecoflex 00-10. We made the membrane bigger than the reflector to overlap it on the front face. The membrane is 0.4-inch-thick and has an overall diameter of 11 inches. We stretch the membrane uniformly over the surface and overlap it with the walls of the reflector. We use rubber bands to secure the membrane against the reflector walls. We stretch the membrane uniformly over the larger diameter to achieve uniform deformation upon application of vacuum.

We performed experiments to determine the value of radial displacement. We measured the depth of the deformed Ecoflex membrane, due to the application of vacuum, for nine different vacuums. For zero vacuum inside the reflector housing, no displacement occurs.

We measured the following depths corresponding to the vacuum levels:

Table 1: This table lists the deflection of the Ecoflex 00-10 membrane for 9 distinct vacuums.

	Vacuum (-kPa)	Deflection (inch)
1	1.89	3
2	1.75	2.917
3	1.61	2.749
4	1.51	2.68
5	1.36	2.489

6	1.27	2.438
7	1.15	2.292
8	1.01	2.11
9	0.78	1.995

2.5 On Axis Acoustical Testing for Gain and Directionality

We implemented an on-axis testing methodology for conducting the gain and directionality trials. We conducted the tests in an outdoor and an indoor environment. The sound source under consideration was a Behritone C50A studio monitor. We used tripods, kept at 1.8m from the ground and 1m apart from each other to support the two systems. We ensured the on-axis alignment using a laser pointer. We used a Behritone studio monitor to output sound using a laptop connected to an NI-DAQ chassis. We used the NI-DAQ chassis to output sine wave from the speaker as well to process voltage data of the B&K microphone.

For the directionality test, we swept through frequencies ranging from 1000 Hz to 10,000 Hz. We produced a sine wave of the corresponding frequency and an amplitude of 0.1V from the speaker using a laptop connected to the speaker. We placed the microphone horizontally at the focus of the parabola. The scale at the base indicated the location of the microphone. We achieved the rotation of the microphone and reflector assembly using a NEMA 23 stepping motor with a torque of 1.7 kN-m. We triggered the stepping motor using an embedded Arduino GRBL code and communicated with using MATLAB/ UGCS (Universal G-code sender). We used a feed rate of ‘1’ while performing the experiments. For instance ‘go1f1y-10’ meant rotating the stepping motor in an anti-clockwise manner

with a feed rate of 1 assuming absolute steps of rotation. We implemented a high pass filter using the MATLAB filter design toolbox with a stop band frequency of 300 Hz and passband Frequency of 400 Hz. We carried out the entire test for 70 seconds and recorded the data using the Bruel and Kjaer microphone. We sampled the data using a sampling rate of 51200. The first two peaks recorded within the processed data indicate start and end of the time vector under consideration. We fitted a sinusoidal wave through the processed and sampled data per frequency.

We recorded the amplitudes of the fitted sine waves in a column vector. We generated a polar plot considering the amplitude of the fitted sine wave per degree of rotation and repeated the procedure for five distinct vacuum levels.

For the acoustic power gain test, we swept through 54 different frequencies ranging from 50 Hz to 10120 Hz on a linear scale. We output every single frequency for one second with a sampling rate of 51200. For a given vacuum and focal length, we experimented with and without the reflector in place. We generate the Acoustic Power Gain (dB) Vs. Frequency (Hz) plot to check the behavior as compared to the theoretical gain of the dish, for seven different vacuum levels. Since we start with 50 Hz, we modify the high pass filter to stop band frequency of 30 Hz and passband Frequency of 40 Hz. For every single frequency, we sampled 45 waves. We fitted a sinusoidal wave through the processed and sampled data per frequency with the fit option given by "a*sin(b*(x)+c)." and recorded a vector with the fitted amplitudes of the sinusoidal waves.

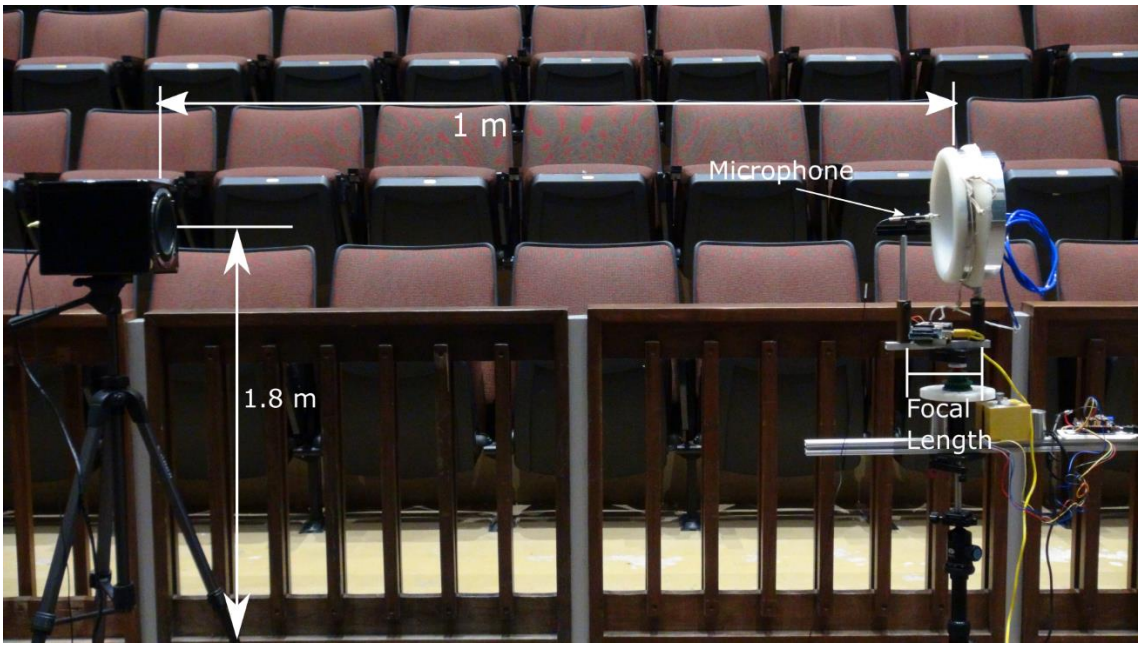

Figure 6: Photograph of the Experimental Setup

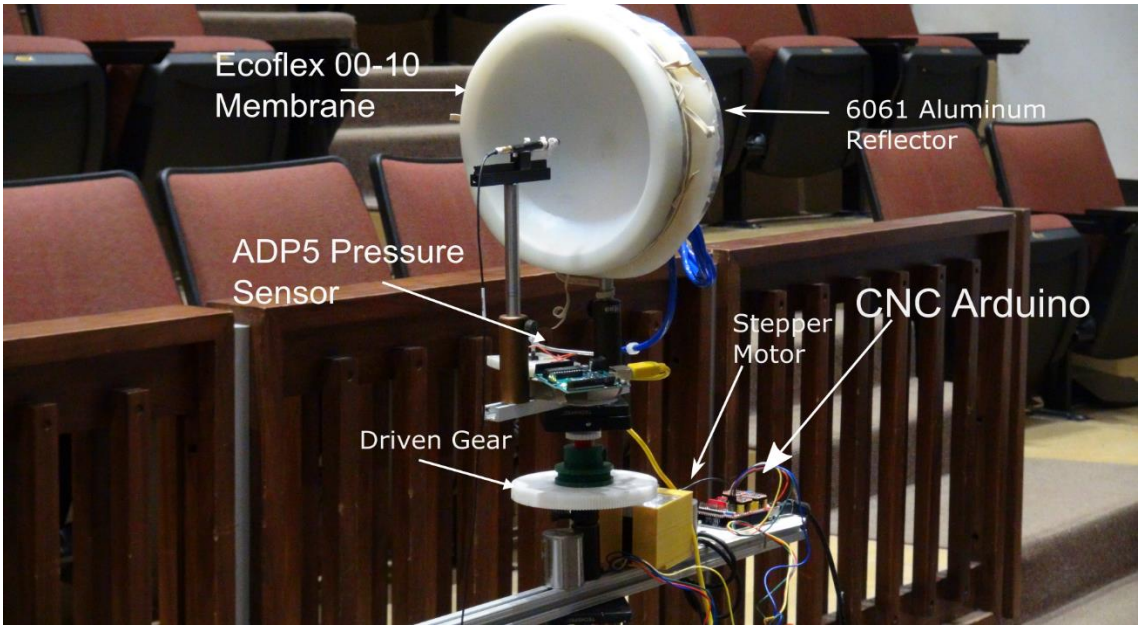

Figure 7: Setup including electronics and pressure sensor

2.6 Fabrication Techniques

2.6.1 3D Printing

The experimental setup comprises of many fixtures, holders, molds and motion transmission components. We use fixtures and holders to hold the microphone, the CNC Arduino board, the Panasonic vacuum sensor and the stepping motor. Since the Nema 23 stepping motor weighs 0.3 kg and exerts a torque of 1.7kN-m on the mating gear, we needed a rigidly fixed base to mount the motor. For rotating the reflector, we implemented the gear-to-gear mesh method. For mounting the vacuum sensor chip, its Arduino board and the associated bred board, we had an additional L- bracket with the peripheries mounted on its base. The stepper motor mount has a ¼''-20 screw-nut glued to the cavity at its base. We fixed the mount of the stepper motor to its base using a ¼''-20 screw-nut. The driven gear has a pitch diameter of 5 inches and has 150 teeth.

The gear ratio is the number of teeth on the driven gear to the number of teeth on the driver gear. The driver gear is a spur gear with a pitch diameter of 0.625 inches and has 20 teeth. Both the driver and the driven gear have a pressure angle of 14.5 degrees. The driver gear has an inner diameter of 0.25 inch. The SI section has the meshed model of the gear-pinion assembly.

The mount for CNC Arduino is a simple 3D printed base plate with dimensions (2.5-inch X 5 inch) and 0.15 inch deep. We used PLA filament with 80% fill to provide extra stiffness. We used a LulzBot TAZ 6 3D printer available at the Rutgers Makerspace. We made use of CURA to set up a 3D printing job.

2.6.2 Laser Cutting for Acrylic

We molded the Ecoflex membrane for the reflecting surface using molds prepared out of acrylic sheets. We used the VLS 2.30 Universal Laser System laser cutter available at the Rutgers Makerspace. We used an acrylic sheet 12'' X 12'' and ¼'' thick for cutting a circular disc 11inches in diameter. We 3D printed a circular ring of thickness 0.4 inch and pasted it on the acrylic base circumferentially to make the mold 0.4 inch deep. It took 20 minutes to cut a single cut disc.

3. COMSOL Based Finite Element Analyses Setup

We validated the results of the gain and directionality experiments by performing Acoustic Finite Element Analyses using COMSOL Multiphysics. COMSOL Multiphysics offers packages within Electromagnetics, Acoustics Structural Mechanics, Heat Transfer, Mathematics, Chemical Species Transport. For our analyses, we made use of the structural mechanics and Acoustics Shell Interaction submodule within COMSOL Structural Mechanics and Pressure acoustic modules.

We implemented the "stationary" study under solid mechanics sub-module. We used this model to solve 2D,3D and axisymmetric bodies. We implement the MUMPS solver and the "Suggested Direct Solver (solid)" as a linear solver. We model the geometry using inch and degrees. We implement the solid mechanic's module to calculate the Young's Modulus of Ecoflex 00-10 and the radial [9]:

$$0 = \nabla . F\, S + F_v \qquad \textbf{(5)}$$

$$F = I + \nabla u \qquad \textbf{(6)}$$

3.1 Cantilever Experiment to determine the Youngs Modulus of Ecoflex 00-10

We initialized the global parameter “e” assigned to the Young’s Modulus. We assigned a blank material to the Ecoflex geometry. We used the specific gravity 1.04g/cc to calculate the density of Ecoflex. We assumed the Poisson's ratio as 0.49. We modeled the geometry of the ecoflex strip as a union of two rectangles. We modeled the material as linear elastic and isotropic and is considered nearly incompressible. We applied a fixed constant to the 0.8-inch length of the strip. The equation of the fixed constraint is $u = 0$. We apply the gravitational load to the rest of the strip whose magnitude given by “-g_const” in the negative Y direction. We implemented “An extremely fine mesh” to the entire domain. Within the study section, we implemented a parametric sweep for the parameter “e”. A probe placed at (2.93, -0.075) gives the displacement of the node.

We swept Young’s modulus E initially in the range 60,000-80,000Pa. We compared the deflection obtained experimentally to that obtained using COMSOL for the given range. We then further swept Young’s modulus in a narrow range from 68000-65000 Pa and further within 68000-67000 Pa to obtain a near to experiment displacement profile.

3.2 Simulation-based determination of Radial Displacement

We verified the nature of the displacement profile obtained post pre-stressing and application of using COMSOL Multiphysics. We modeled the membrane as a union of two cylinders, one with an OD of 11 inches and the other with an OD of 9 inches. We assigned the membrane a blank material with the properties of Ecoflex and the value of Young's Modulus obtained from the cantilever experiment. We modeled the material as a linear elastic isotropic material. We initially swept through a range of values for radial displacement, starting 0.1 to 2mm with an increment of 0.1mm. The vacuum under consideration was -1.51 kPa. A probe placed at (0,0,0.3), snapped to the closest boundary was under for measuring the displacement in inches. The probe measured the displacement and the geometry frame of reference X_g, Y_g, Z_g considered. We prescribed the outer boundaries with fixed constraints. The boundaries of the inner cylinder have a prescribed displacement constraint on them given by:

$$u_0 x = \frac{(Rd * x)}{\sqrt{x^2 + y^2}} \quad \textbf{(7)}$$

$$u_0 \mathrm{y} = \frac{(Rd * y)}{\sqrt{x^2 + y^2}} \quad \textbf{(8)}$$

We made use of a cut line in the form of a line segment bounded by (-4.5,0,0) and (4.5,0,0) to plot the profile of the deformed membrane on a 2D graph. The data generated by the cut line represents the displacement in inches over the cut line.

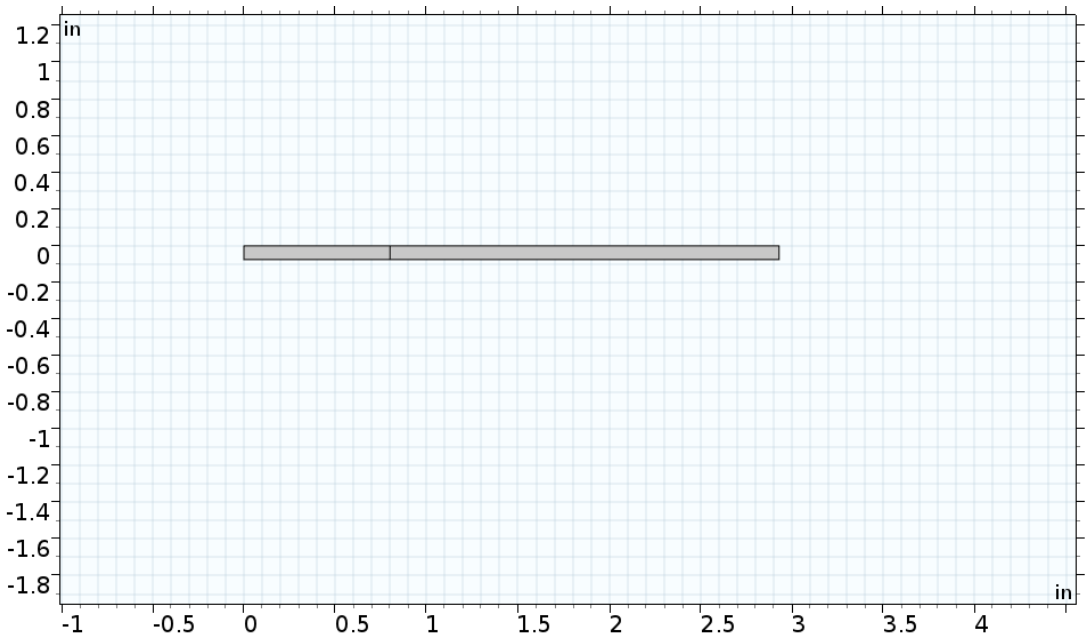

Figure 8: Ecoflex strip modeled as a union of two rectangles.

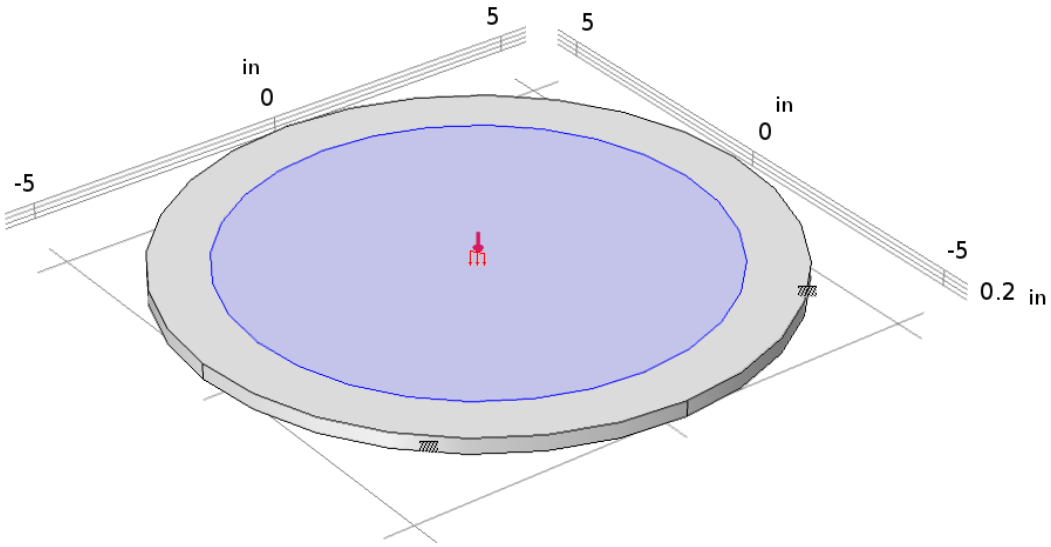

Figure 9: Ecoflex membrane modeled as a union of two cylinders in COMSOL. We fixed the boundaries of the outer cylinder and applied pressure load to the top surface of the inner cylinder.

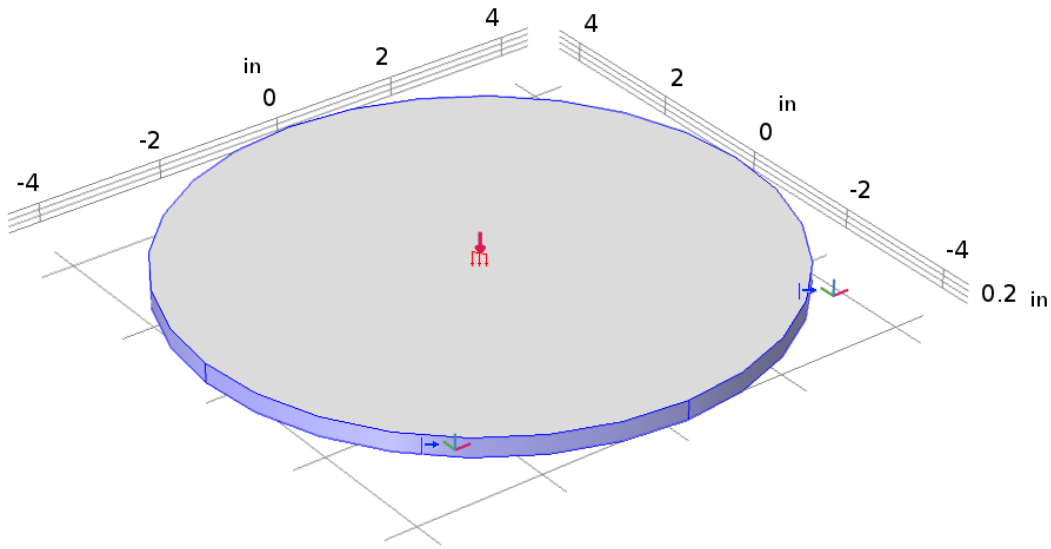

Figure 10: Ecoflex membrane modeled as a union of two cylinders in COMSOL. We fixed the boundaries of the outer cylinder and applied pressure load to the top surface of the inner cylinder.

3.3 Simulation Setup

For validating the nature of the results obtained experimentally we simulated an ideal case. The main elements of the simulation were the acoustic parabolic reflector, speaker, and domain under consideration. We used the Acoustic Shell interaction submodule to model the simulation implementing 3D domains[10]:

$$\nabla\left(\frac{-1}{\rho_c}(\nabla p_t - q_d)\right) - \frac{k_{eq}^2 * p_t}{\rho_c} = Q_m \quad \textbf{(9)}$$

$$p_t = p + p_b \quad \textbf{(10)}$$

$$k_{eq}^2 = \frac{\omega^{\,2}}{\omega_c^2} \quad \textbf{(11)}$$

Where k_{eq} is the equivalent wave number, p_t is the total pressure, which also the sum of background and scattered pressure. q_d and Q_m are the dipole and monopole sources. We couple the pressure acoustics with shell mechanics at the interface. The coupling involves the fluid load on the structure and the acceleration experienced by the fluid due to structure.

The following equation for acoustic-structure interface [10]:

$$-\mathrm{n}.\left(\frac{-1}{\rho_c}(\nabla p_t - q_d)\right) = -n.u_{tt} \quad \textbf{(12)}$$

$$F_A = p_t.n \quad \textbf{(13)}$$

U_{tt} the structural acceleration, n is the surface normal; p_t is the total acoustic pressure. The reference pressure is 20µPa. We model the domain as 4m in diameter, and the medium inside as linear elastic. The ambient temperature is 293.15 K. We modeled a PML (Perfectly Matched Layer) of thickness one-third that of the wavelength outside the domain. We applied a pressure of 0.1 Pa on the diaphragm of the speaker.The equation of this boundary condition is $p_t = p_o$ .We modeled the remaining boundaries of the speaker as interior sound hard boundaries. The equations for this boundary condition are[10]:

$$-\mathrm{n}.\left(\frac{-1}{\rho_c}(\nabla p_t - q_d)_{up} = 0 \right. \quad \textbf{(14)}$$

$$-\mathrm{n}.\left(\frac{-1}{\rho_c}(\nabla p_t - q_d)_{down} \right. \quad \textbf{(15)}$$

$$= 0$$

While performing simulations, we imported the ".stl" file of the deformed geometry of the reflector. We implemented a user-defined mesh with quad elements for air, reflector and speaker domains and swept elements (with five elements per wavelength) for the PML. The maximum size of the element was one-third that of the wavelength and the minimum size was 0.001 m.

We solved the model to obtain the acoustic pressure at a point. We recorded the pressure and Sound Pressure Level using a probe placed at the focus of the parabola.

3.4 Parabolic Reflector Geometry

We sketched the profile of the membrane in COMSOL using a bezier polygon and further rotated it about its axis to form a solid. The membrane is then pre-stressed by applying a prescribed displacement.

$$u_0\mathrm{x} = \frac{(Rd * x)}{\sqrt{x^2 + z^2}} \quad \textbf{(16)}$$

$$u_0\mathrm{z} = \frac{(Rd * z)}{\sqrt{x^2 + z^2}} \quad \textbf{(17)}$$

We applied a pressure load on the boundary of the inner cylinder. A probe placed at (0,0.35) has the expression “solid.disp” and records the displacement of the membrane. The solved model is “Re-meshed” for its deformed contours. We then save the re-meshed model of the deformed contour as a “.stl” file.

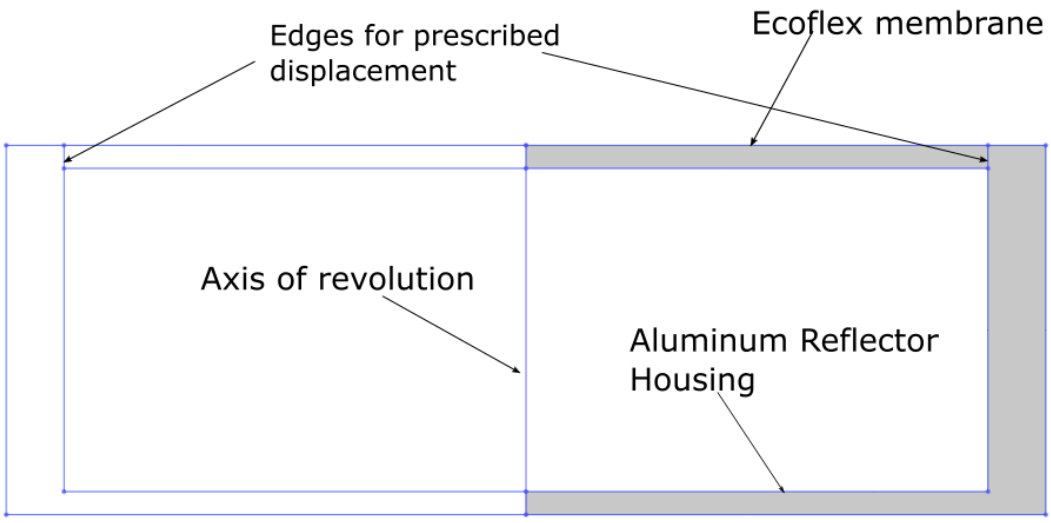

Figure 11: 2D sketch of the Aluminum Reflector housing. The 2D sketch is the converted into a solid to form a domain. We revolve the solid around the axis to form the reflector

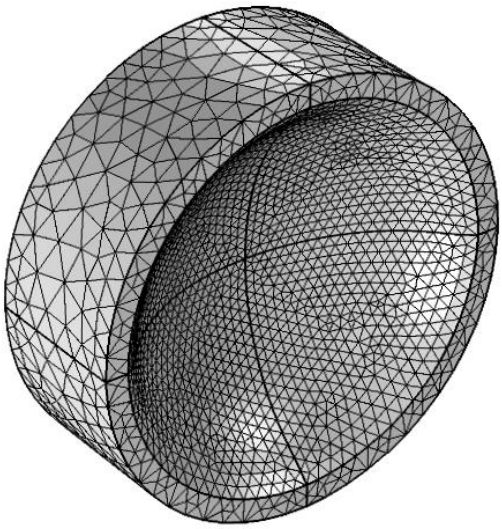

Figure 12: The image is that of the deformed and re-meshed geometry of the reflector. The reflector is pre-stressed along the circumference of the inner diameter and applied a vacuum of -1.5 kPa.

3.5 Impedance Boundary Conditions

The impedance boundary condition relates the acoustic pressure and acoustic velocity to each other at a given point. We impose the impedance boundary conditions on a material to differentiate it from sound hard material and a soft sound material. For pressure acoustics, the boundary condition is as follows[10]:

$$-\mathrm{n}.\left(\frac{-1}{\rho_c}(\nabla p_t - q_d)\right) = -\frac{i * \omega * p_t}{Z_i} \quad \textbf{(18)}$$

Where; Z_i is the transfer impedance in (Pa*s/m).

$$Z_i = \frac{\Delta p}{v} \quad \textbf{(19)}$$

Experimentally, Normalized boundary specific impedance is[11]:

$$\frac{z}{\rho_o * c} = \frac{1 + r}{1 - r} \quad \textbf{(20)}$$

Where r is:

$$r = \frac{H_{12} - e^{-jk_0 s}}{e^{jk_0 s} - H_{12}} * e^{2jk_0 x_1} \quad \textbf{(21)}$$

Where; x_1 is the distance between the test sample and the further microphone. K_0 is the specific wave number and given by

$$k_0 = \frac{2 * \pi * f}{C_0} \qquad \textbf{(22)}$$

C_0 is the speed of sound.

We took into consideration the data obtained from the impedance tube experiment performed by Yanjun and Robert Foster[7]. We extrapolated the transfer function H_{12} impedance tube experiment to 10,000 Hz. Originally the experiment was performed for frequencies within the range 300 to 4500 Hz.

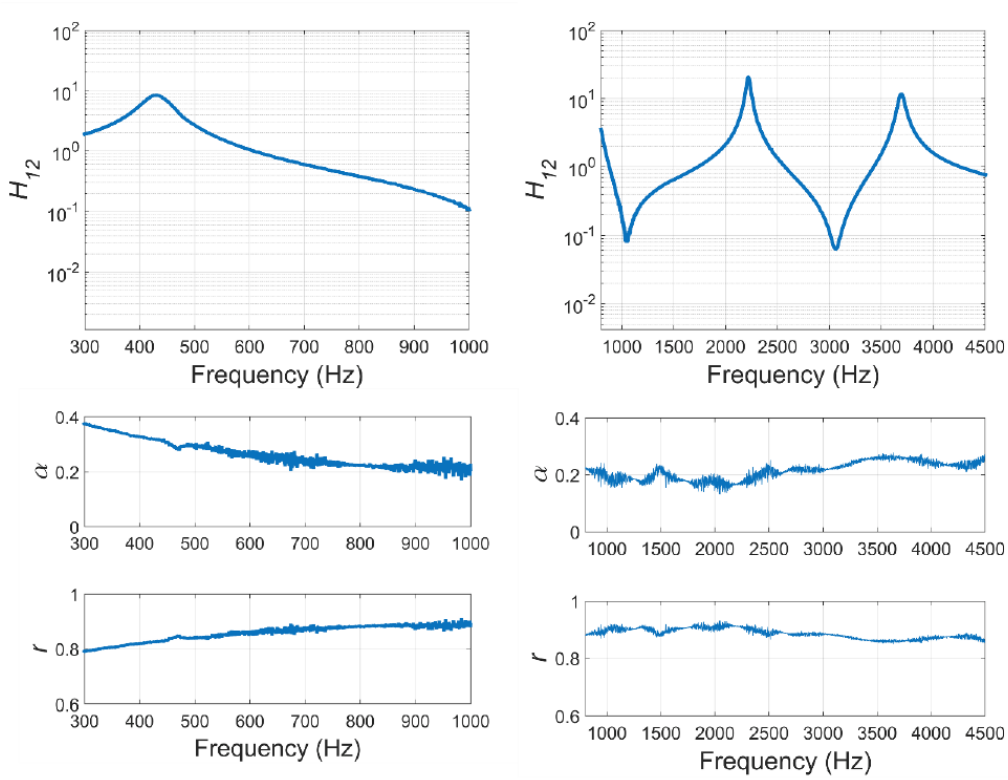

Figure 13: Absorption and reflection coefficients of a 20-mm thick Ecoflex 00-10 sample[7].

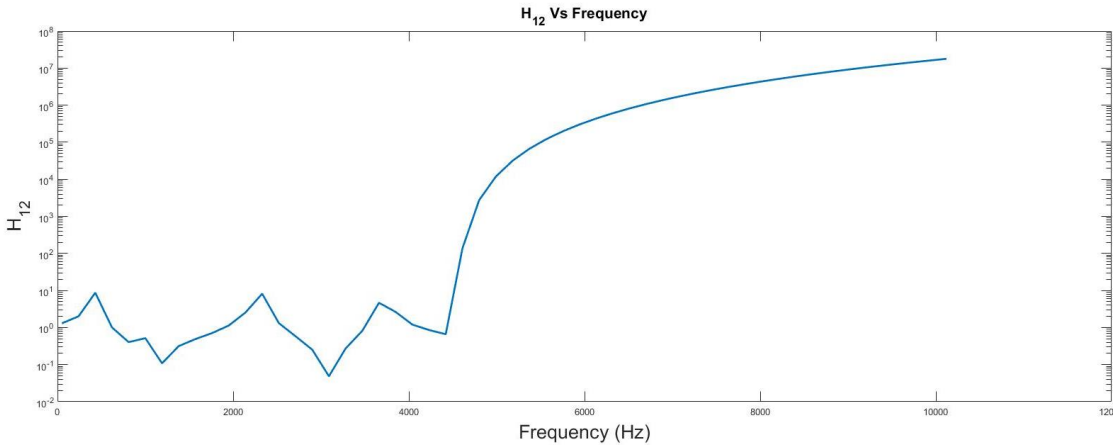

Figure 14: Extrapolated Plot for H_{12} considering data available from the impedance tube experiment from frequencies ranging 300 Hz- 4500 Hz[7].

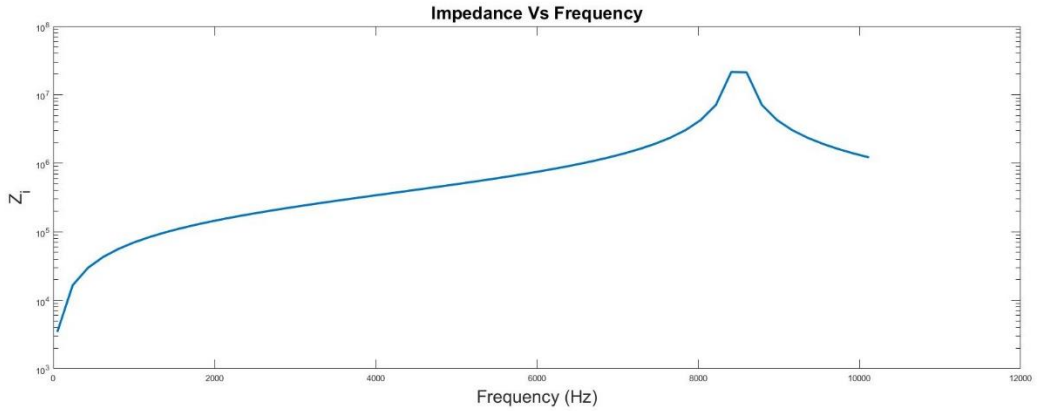

Figure 15: The above plot represents the distribution of Specific Impedance values over frequencies ranging 100 Hz to 10120 Hz.

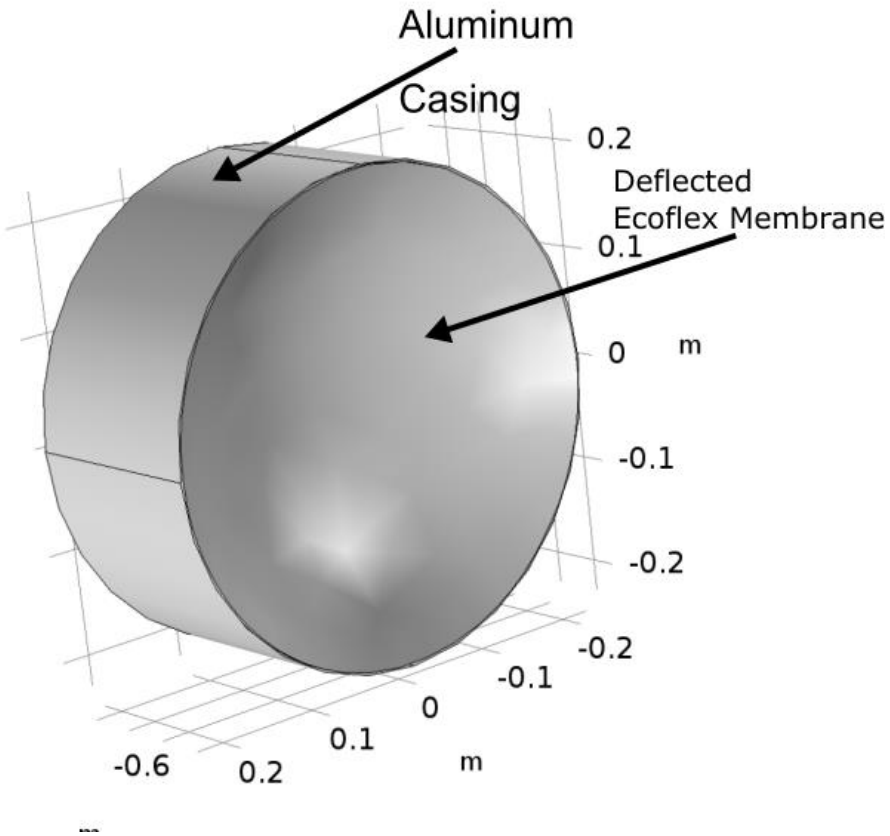

Figure 16: Reflector Housing comprising of Aluminum housing and Ecoflex reflecting surface

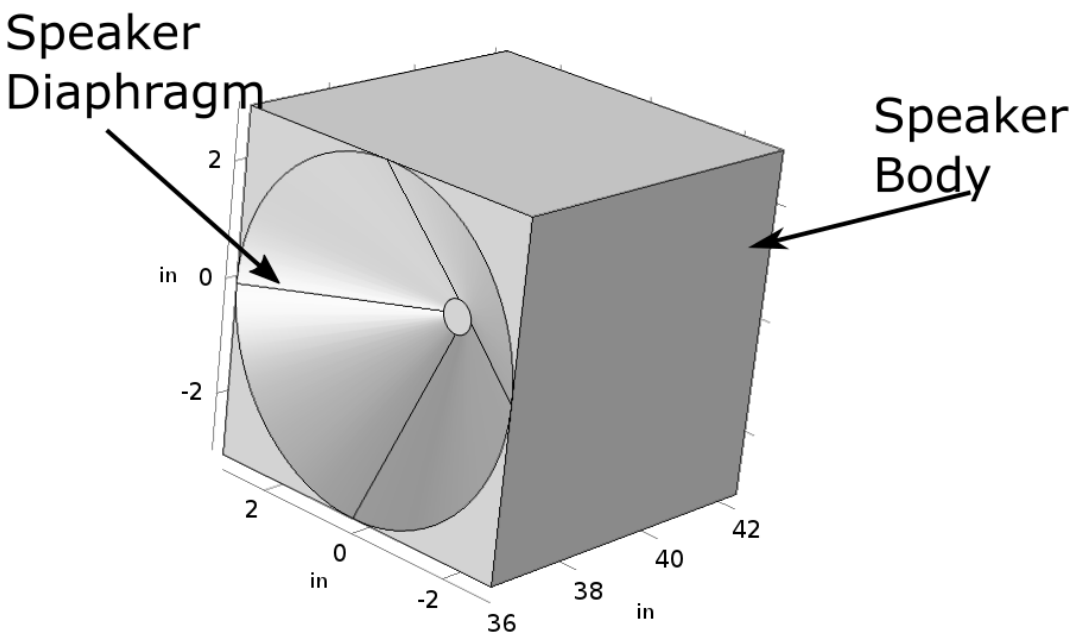

Figure 17: Speaker domain which comprises the plastic body and titanium diaphragm.

4. Results and Conclusion

4.1 Membrane Mechanics

4.1.1 Determination of Young's Modulus

We consider the Ecoflex 00-10 as a linear elastic material. We made use of the structural mechanic's module within COMSOL to obtain deflections. We suspended the Ecoflex strip for a single length of the suspension. Figure 20 shows the suspended profile of Ecoflex 00-10. We measure the total deflection to be 2.17 inches from the horizontal datum.

We divided the Ecoflex strip into two subdomains. The first part represented the fixed portion of the strip and the latter the suspended portion of the strip. The free portion of the strip deflected due to self-weight. We used the MATLAB function; infuse(a,d,'blend', 'Scaling,' 'joint'); to overlay the experimental photo over that obtained using simulation.

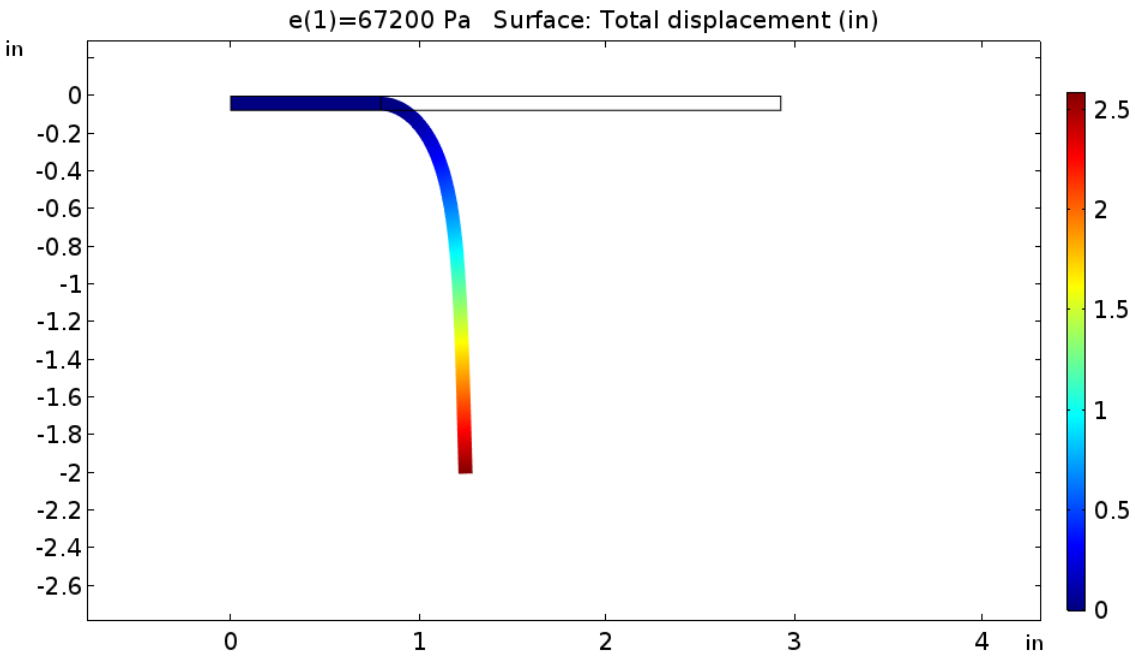

Figure 18: A plot for the total deformation of the Ecoflex strip suspended as a cantilever obtained using COMSOL.

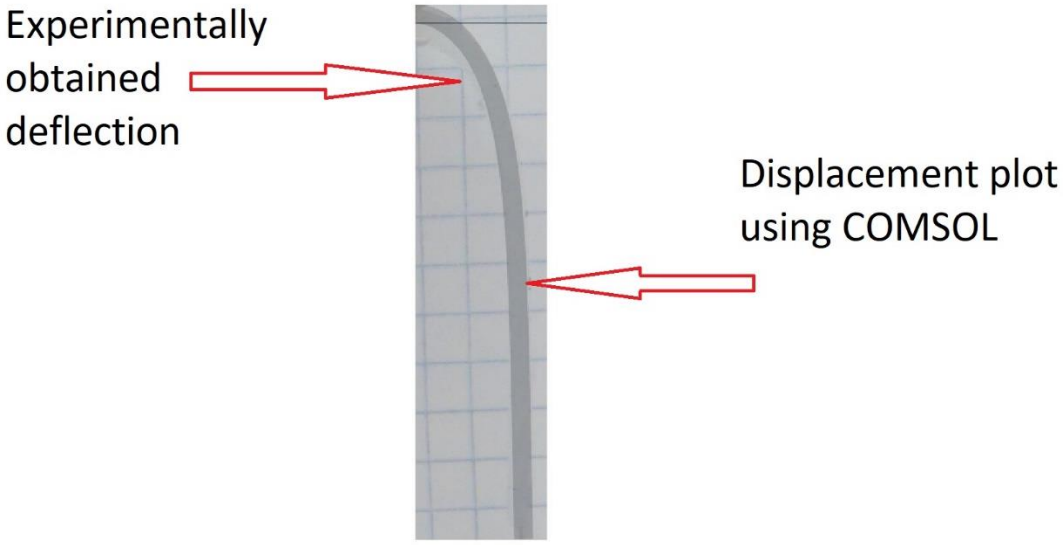

Figure 19: An overlaid image which compares the experimentally obtained Ecoflex profile and the profile obtained using COMSOL simulation.

We calculated the Young's Modulus of Ecoflex 00-10 to be 67.2kPa.

4.1.2 Experimental determination of Radial Displacement

We stretched the membrane uniformly over the outer diameter, thus pre-stressing it. We made use of the solid mechanics module while calculating the radial displacement. Due to the prescribed displacement boundary conditions, the membrane records some initial displacement without any application of load. We measured the depths of the membrane for nine different vacuum levels and found out that for a radial displacement of 0.6 mm the depth recorded using COMSOL matched that recorded experimentally.

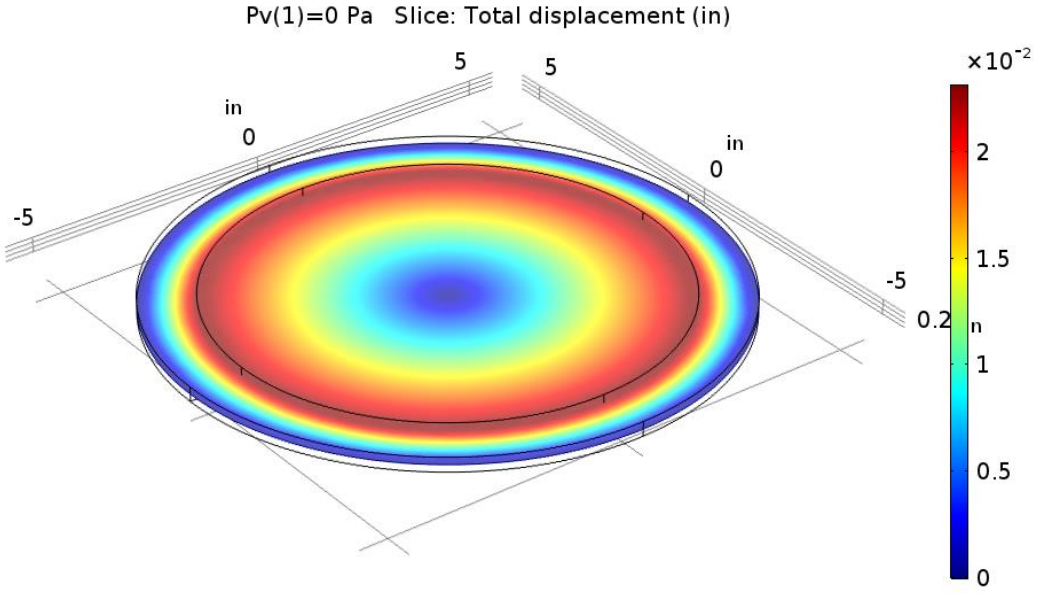

Figure 20: Displacement profile of the membrane upon application of initial prescribed displacement. The probe records minor displacement even though there is no pressure load on the top surface.

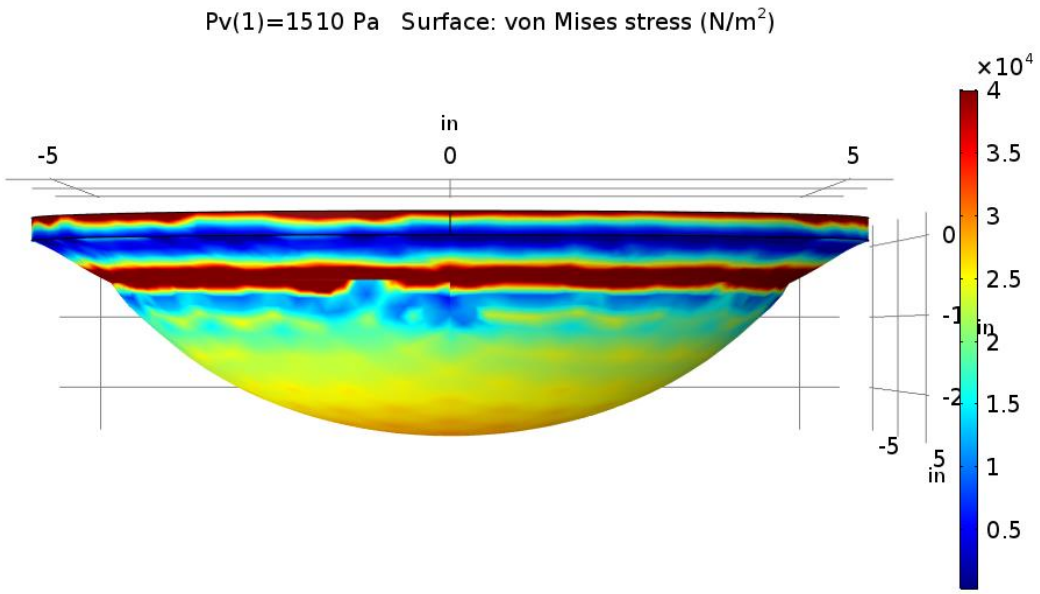

Figure 21: Stress distribution over the surface of the membrane after its prestressed and applied a surface pressure load of -1.51 kPa.

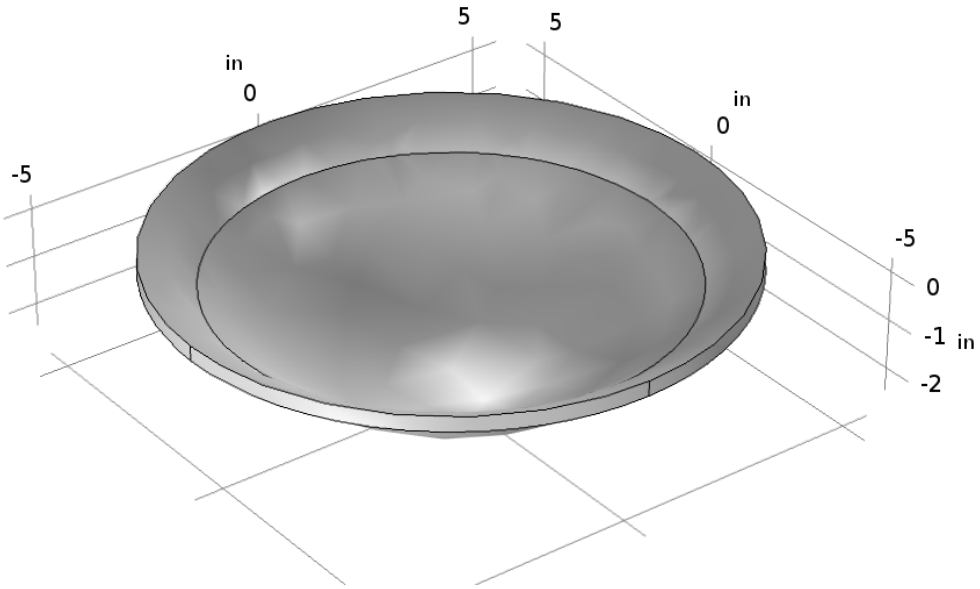

Figure 22: Deformed contour of the membrane obtained after it has been pre-stressed and applied a vacuum load of -1.36 kPa.

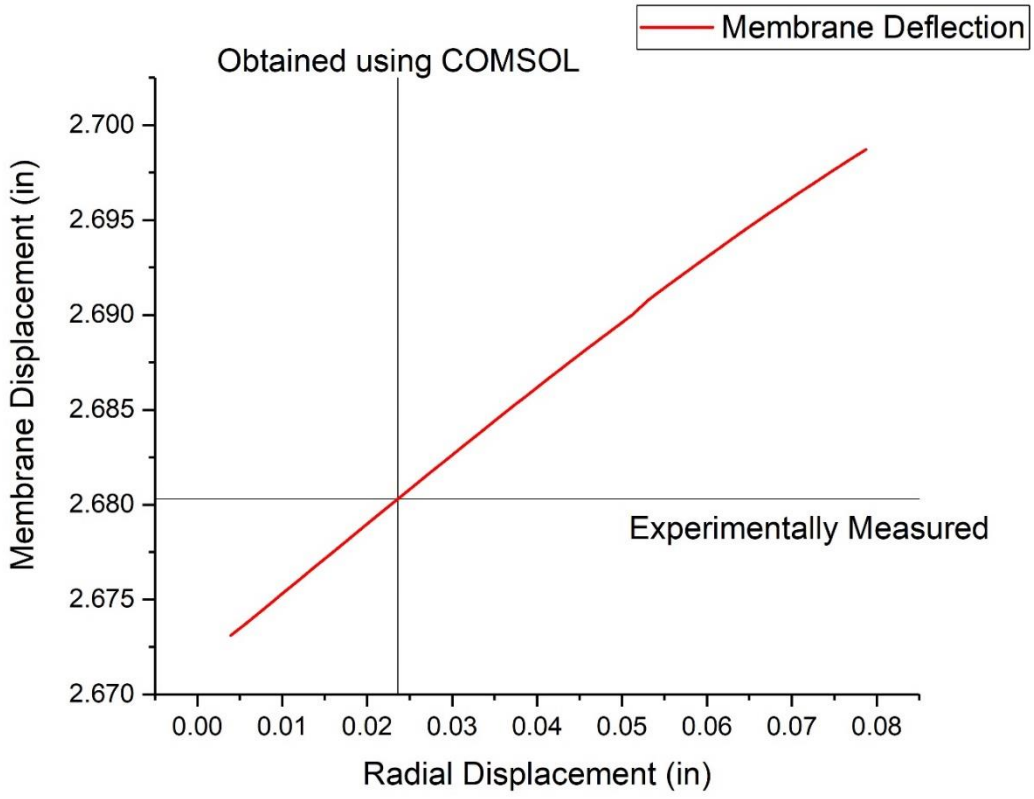

Figure 23: Membrane deflection obtained per 0.1 mm increment in radial displacement using COMSOL Multiphysics. We performed the simulation for -1.51 kPa.

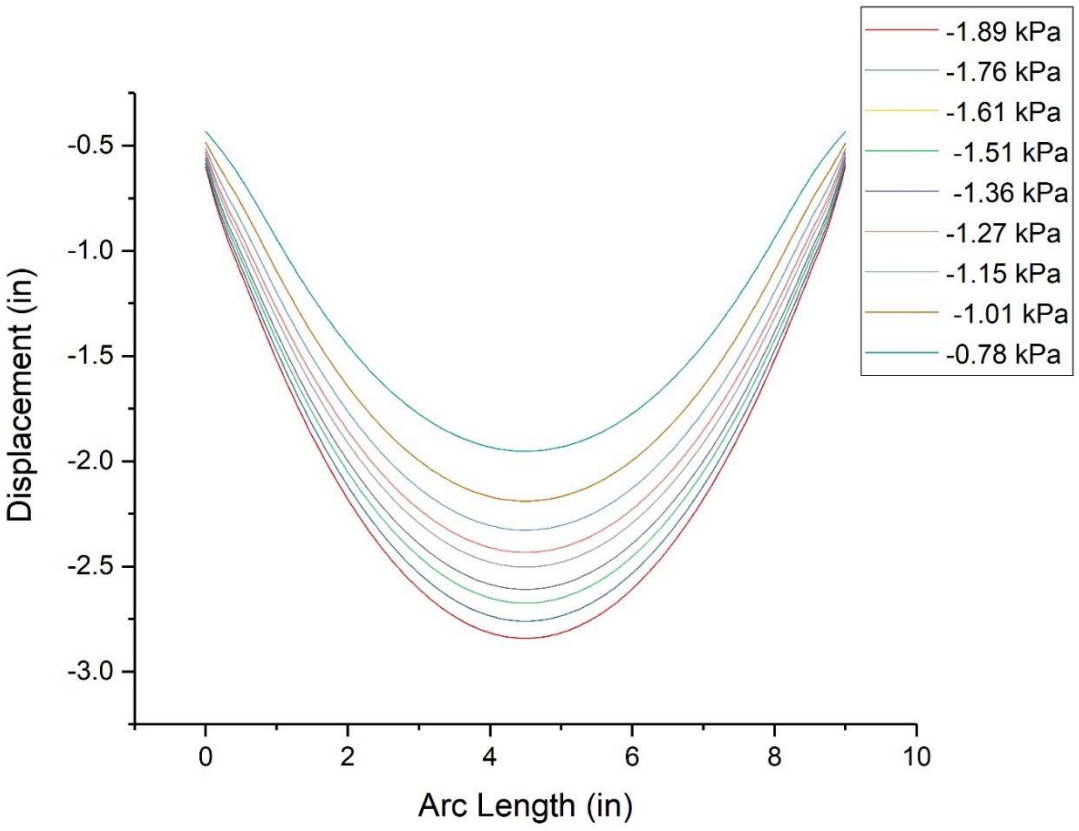

Figure 24: Plot for displacement profiles obtained using COMSOL for nine different vacuums and a radial displacement of 0.6 mm.

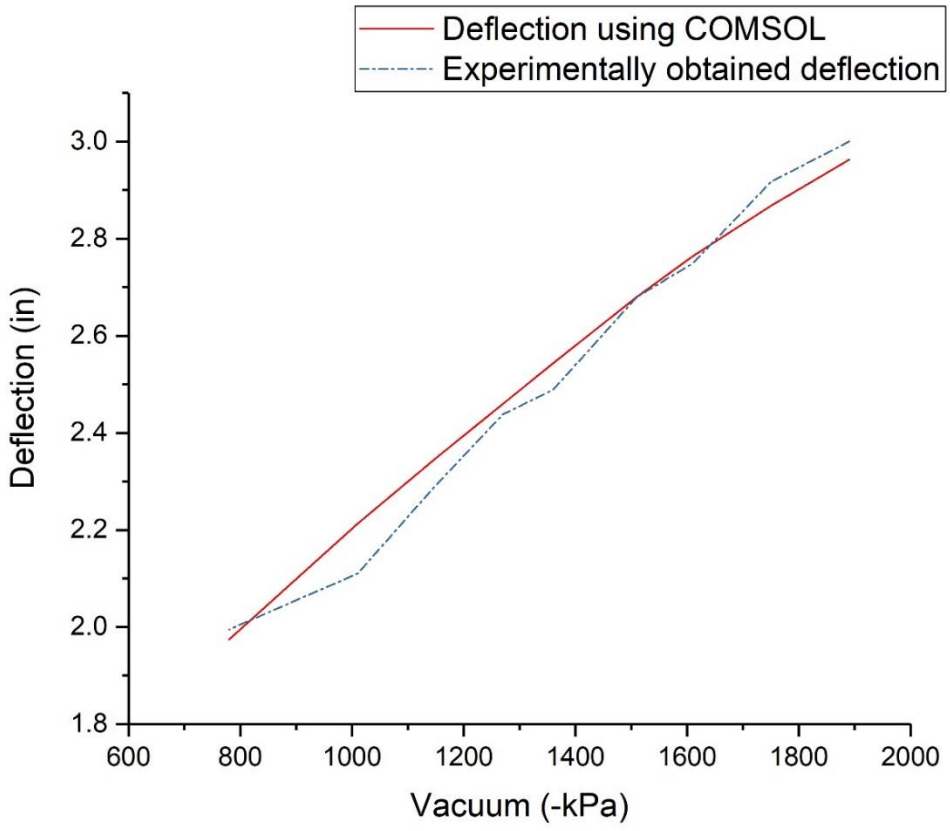

Figure 25: The figure consists of the plot for deflection vs. vacuum obtained using COMSOL overlaid with the plot obtained experimentally.

For a 0.6 mm radial displacement, the plot obtained using COMSOL agrees with that obtained experimentally.

4.2 Experimental Acoustic Power Gain

The parabola formed due to pulling vacuum from the reflector housing focuses the sound energy incident upon it at the focus. The acoustic parabolic gain of the dish is directly proportional to the logarithm of the dish area and inversely proportional to the logarithm the wavelength. While performing the gain trial, we swept for 54 different frequencies ranging from 50 to 10120 Hz on a linear scale. We generated sound, in the form of sine waves using MATLAB and output it from a Behringer C250 Studio Monitor. The corresponding MATLAB command used is [data(loop_now,:),time] = s.startForeground();

The process code first applies a highpass filter to the data and fits a sine wave passing through it. The experimental Acoustic Power Gain of the signal is[12]:

$$P(dB) = 10 * \log_{10} \frac{\mathrm{P}}{P_r} \qquad \textbf{(23)}$$

Where; Pr is the reference power in Watt. While experimenting, we considered the reference power as that measured without the reflector in place. The microphone has an output in volts, and its sensitivity is 60 mV/Pa[13]. The amplitude of the fitted sine wave represents the voltage recorded by the microphone for a given frequency. After implementing voltage to pressure conversion, the modified expression of Acoustic Power gain is:

$$P(dB) = 20 * \log_{10} \frac{\mathrm{V}}{V_r} \qquad \textbf{(24)}$$

Where; V_r is the reference voltage recorded for the corresponding frequency when the reflector is not in place. We performed the experiment for 4 different vacuums, -1.91 kPa, -1.72 kPa, -1.52 kPa and -1.01 kPa. We observe that for higher frequencies, as the vacuum in the reflector increases the gain also increases. Fig 25,26,27 indicate the effect of the application of a high pass filter.

Freq: 240 Hz

Without Reflector Plot:

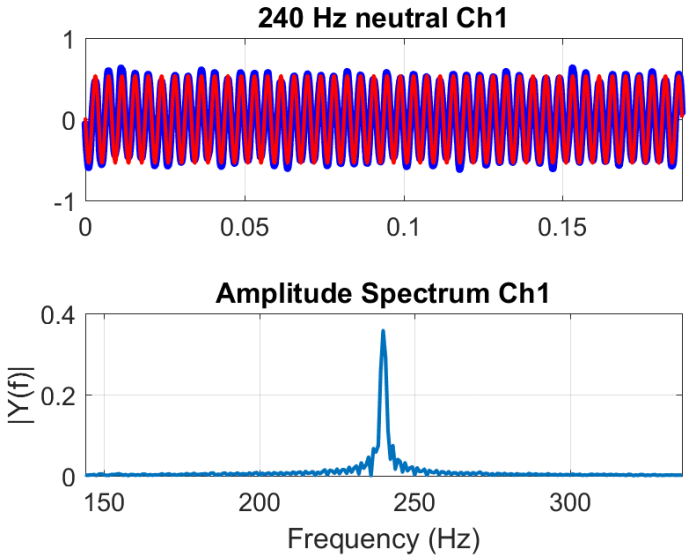

With Reflector Plot:

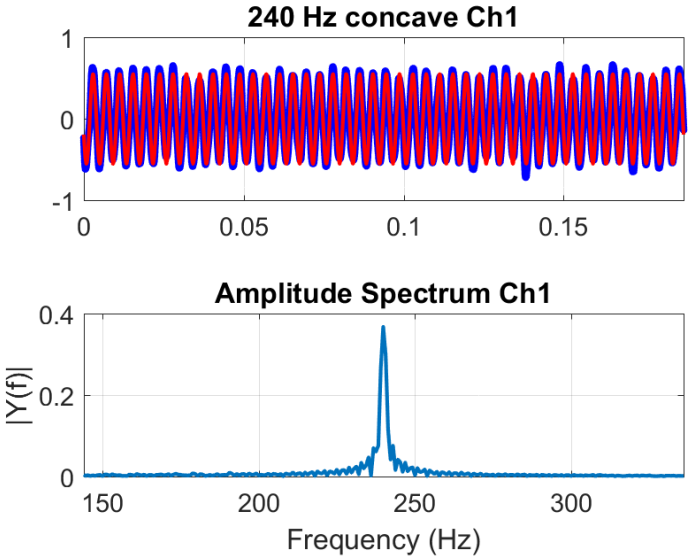

Figure 26: Subplot 1 contains a fitted sine wave against the data processed using the microphone for 240 Hz. Subplot 2 indicates the amplitude of the fitted sine wave obtained by performing an FFT of the data generated using a microphone.

500 Hz With Reflector Plot:

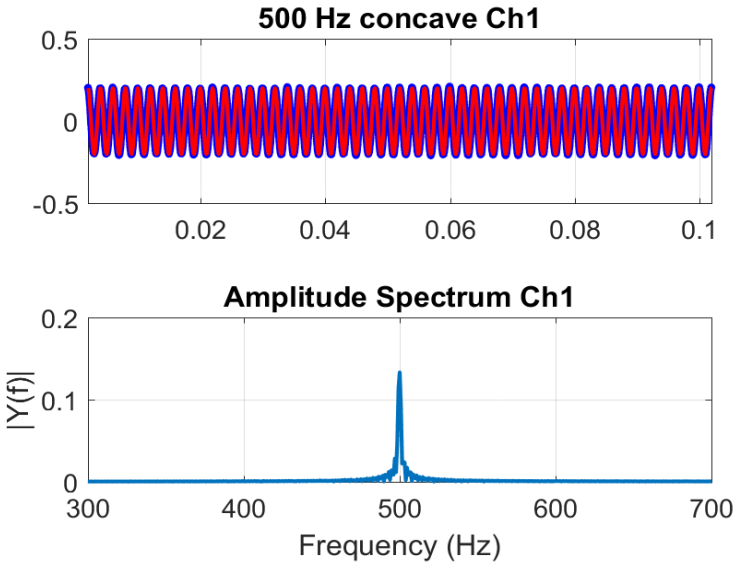

500 Hz Without Reflector Plot:

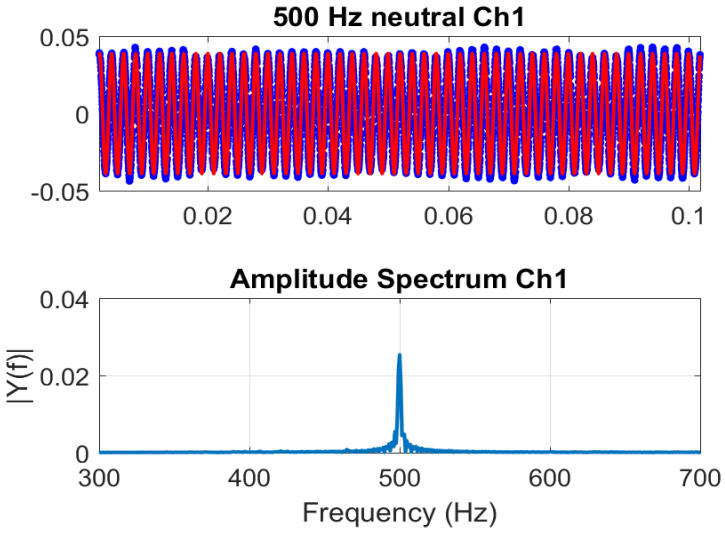

Figure 27: Subplot 1 contains a fitted sine wave against the data processed using the microphone for 500 Hz. Subplot 2 indicates the amplitude of the fitted sine wave obtained by performing an FFT of the data generated using a microphone.

Freq: 4300 Hz

Without Reflector Plot:

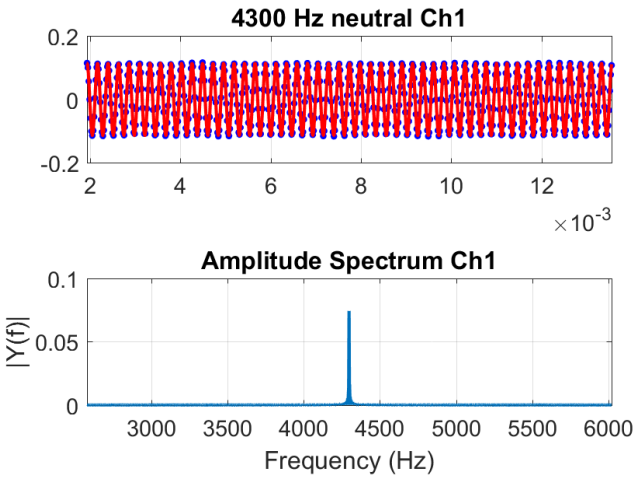

With Reflector Plot:

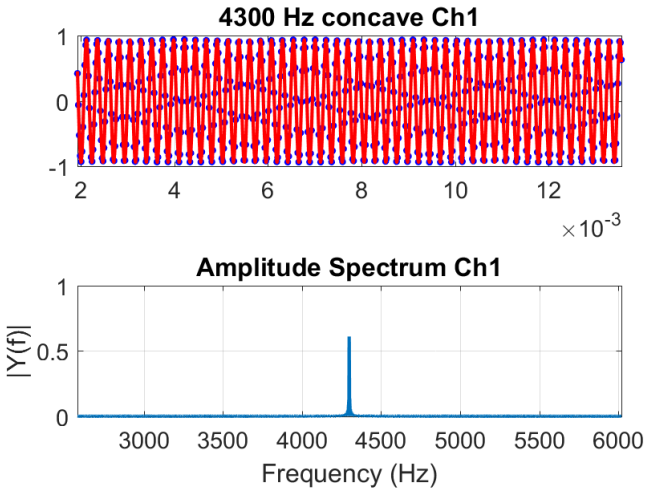

Figure 28: Figure: Subplot 1 contains a fitted sine wave against the data processed using the microphone for 4300 Hz. Subplot 2 indicates the amplitude of the fitted sine wave obtained by performing an FFT of the data generated using a microphone.

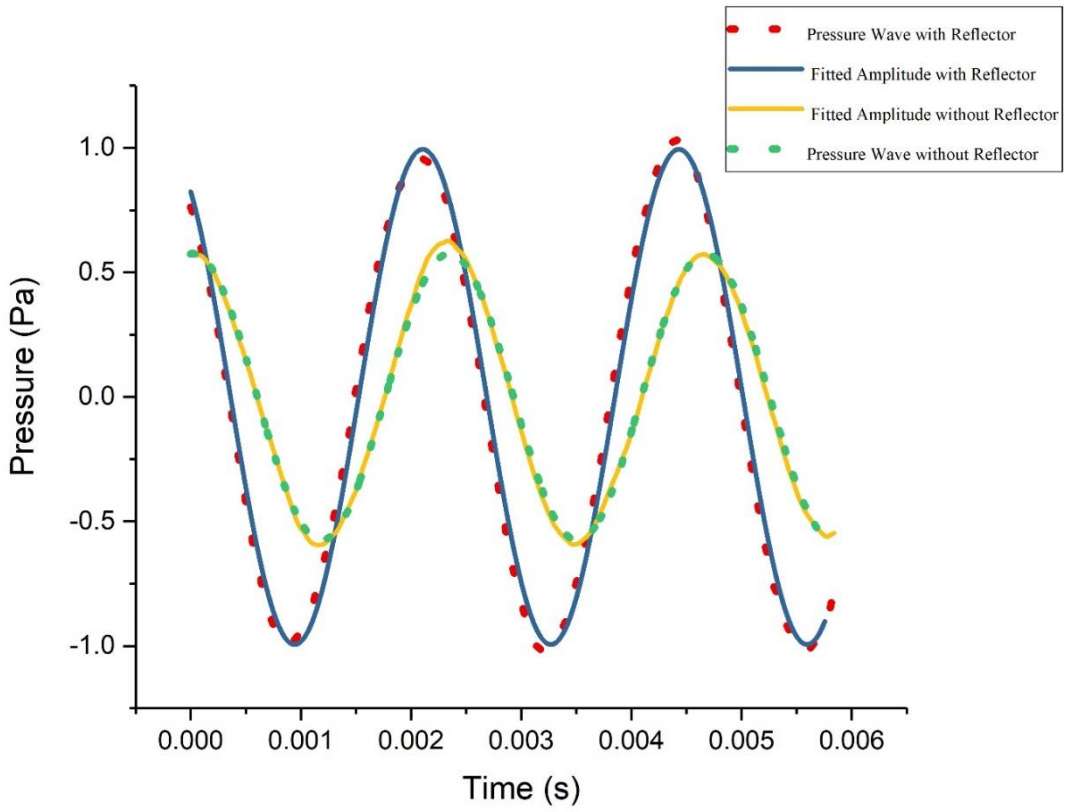

Figure 29: We plot the amplitude of the fitted sine as well as the pressure wave data wave when the reflector is present against the amplitude of the sine wave when the reflector is not present for 430 Hz. We sampled two waveforms. We made use of the amplitudes of the fitted sine waves further to calculate the experimental acoustic power gain.

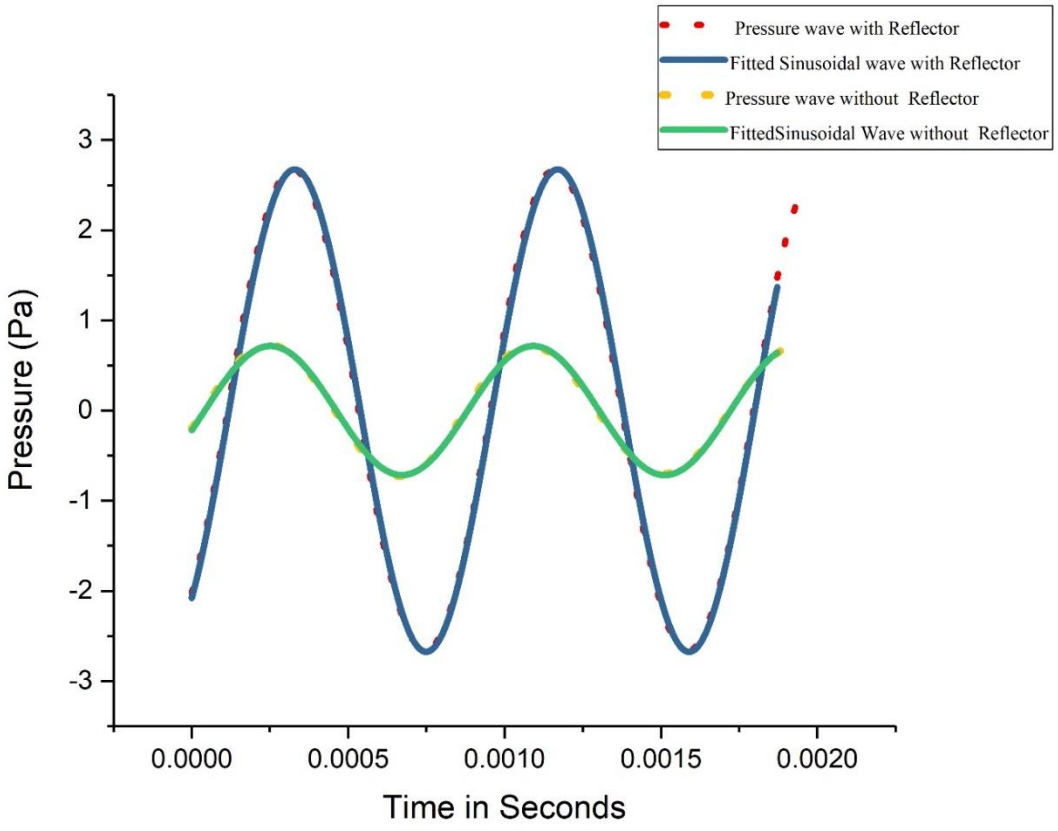

Figure 30: We plot the amplitude of the fitted sine wave as well as the pressure wave data when the reflector is present against the amplitude of the sine wave when the reflector is not present for 1190 Hz. We made use of the amplitudes of the fitted sine waves further to calculate the experimental acoustic power gain.

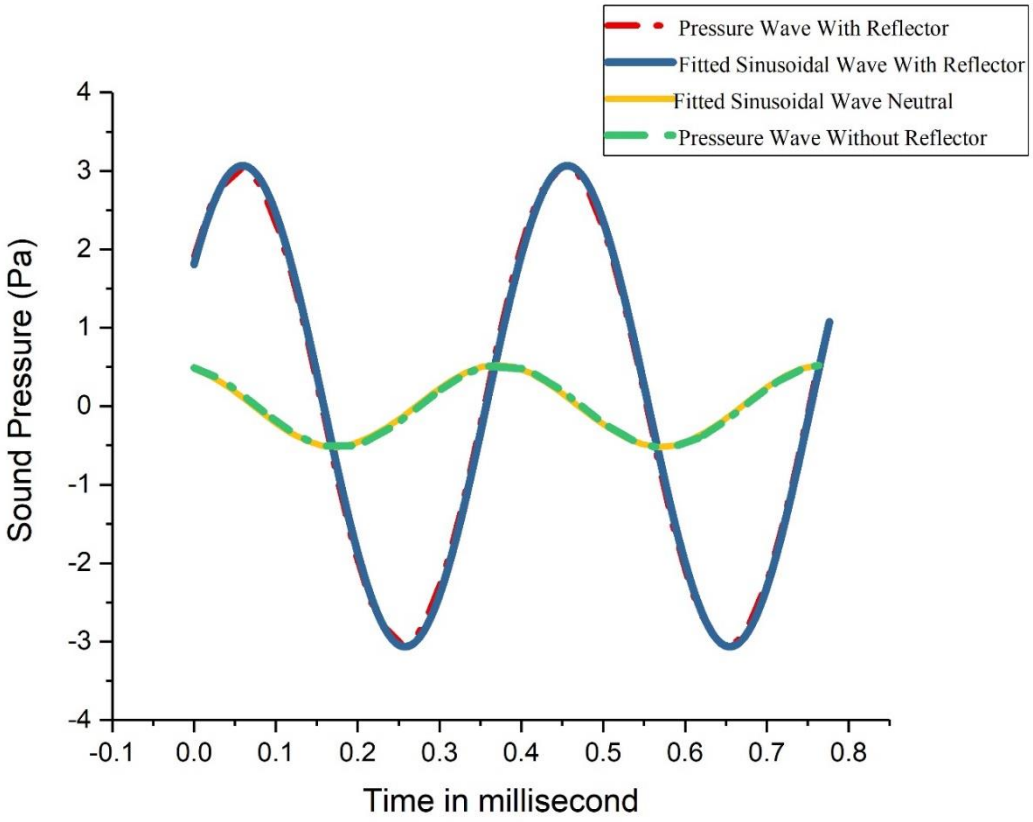

Figure 31: We plot the amplitude of the fitted sine wave as well as the pressure wave data when the reflector is present against the amplitude of the sine wave when the reflector is not present for 2520 Hz. We made use of the amplitudes of the fitted sine waves further to calculate the experimental acoustic power gain.

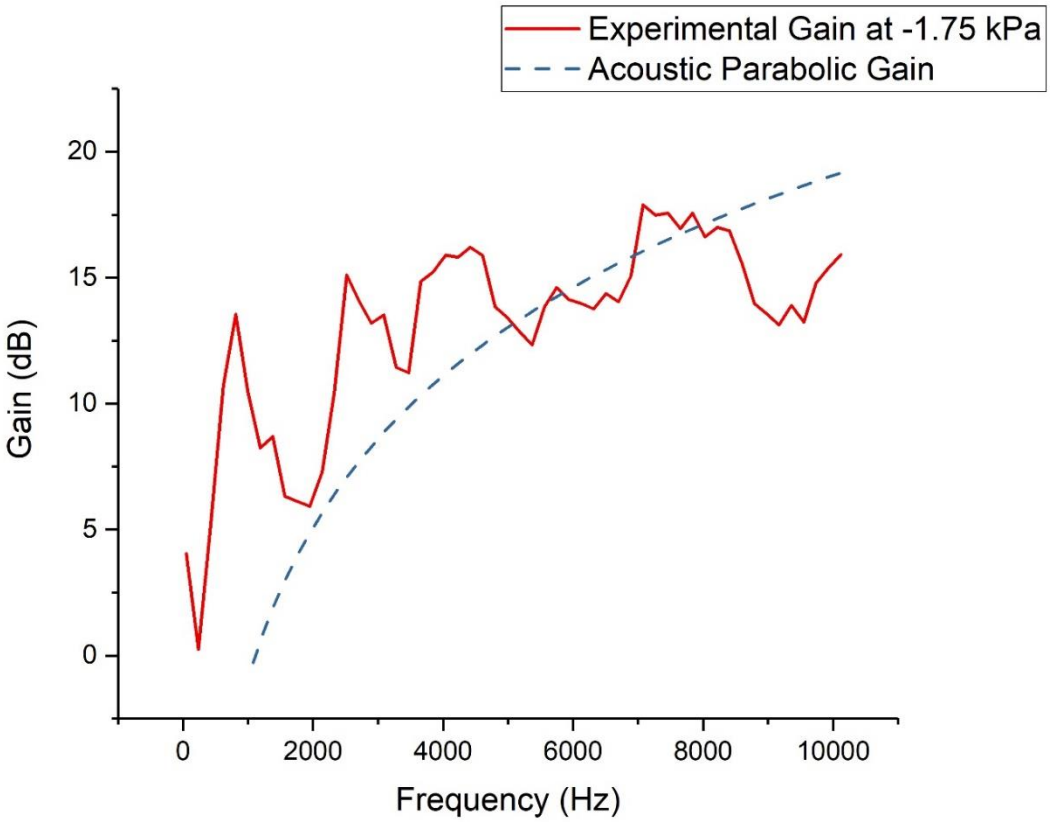

Figure 32: The above graph has plots for Experimentally obtained Gain (dB) and that for the acoustic parabolic gain for 54 different frequencies between 50 Hz and 10120 Hz. We fit the acoustic parabolic gain which is a function of wavelength and dish diameter against the experimental gain. The efficiency of the dish is 42.61%, calculated using the curve fitting parameter.

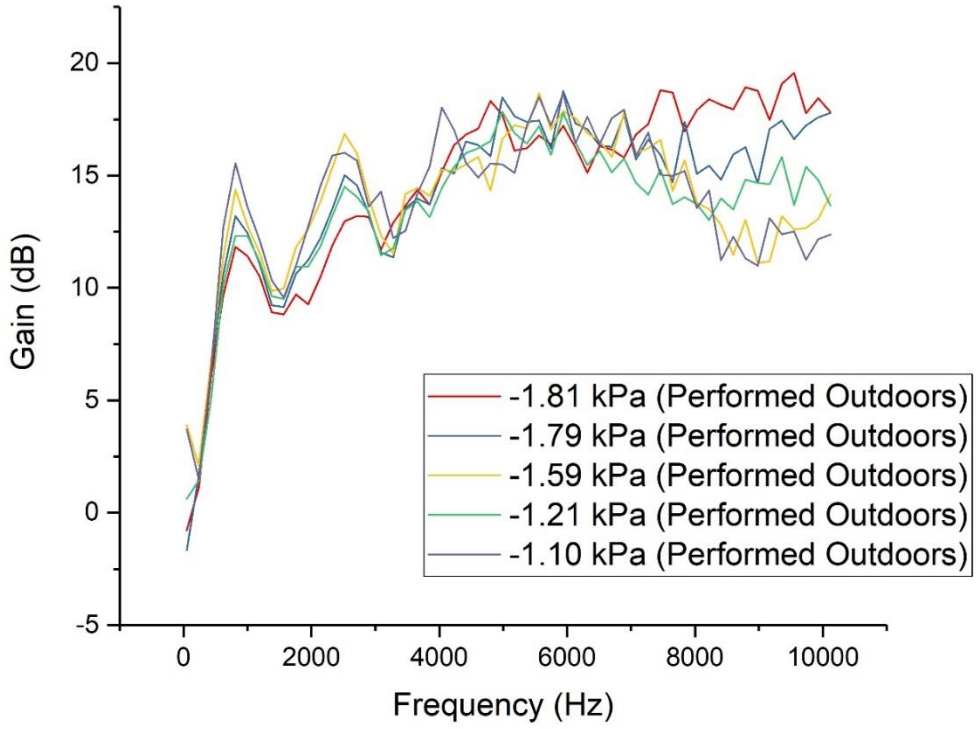

Figure 33: We plot the experimental acoustic power gain obtained for five different vacuums for frequencies ranging 50 Hz to 10,120 Hz for experiments performed outdoors.

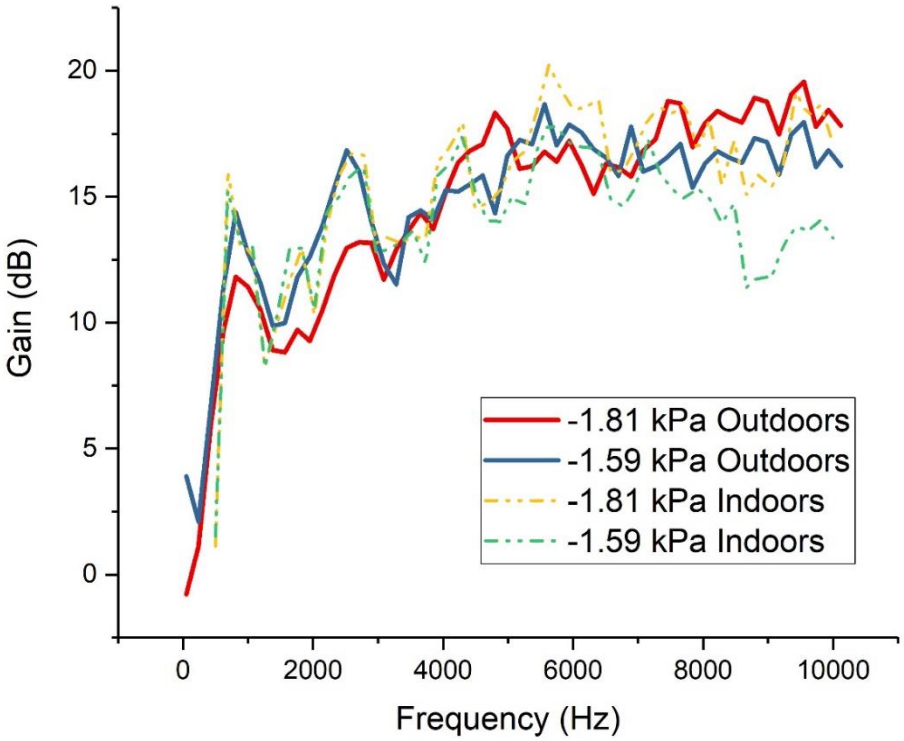

Figure 34: The above plot compares the Experimental Acoustic Power Gain from experiments performed outdoors and Indoors.

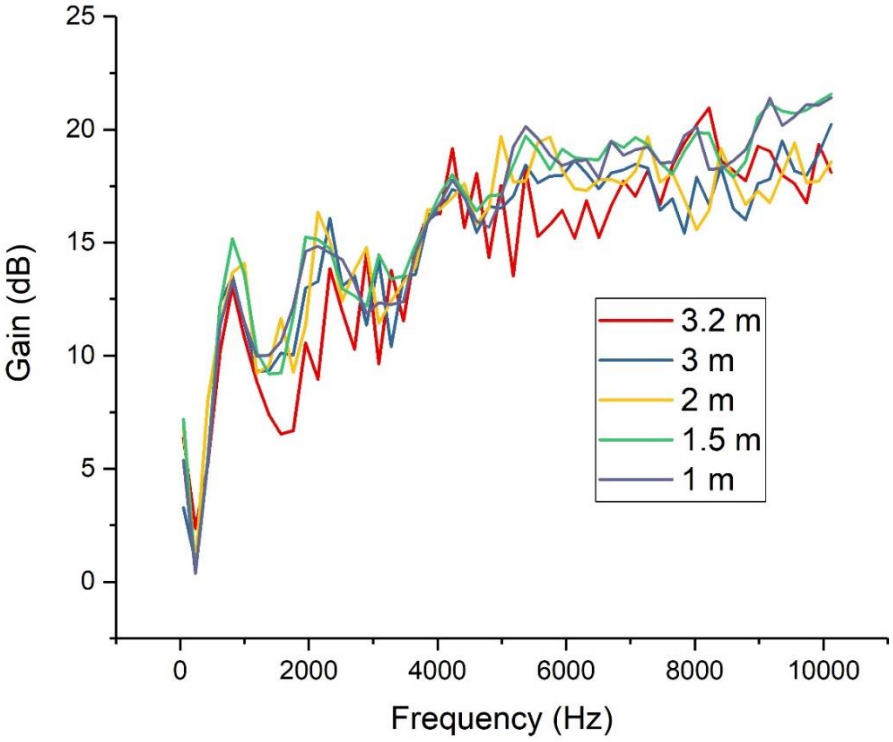

Figure 35: The graph indicates variation in the gain plot by changing the distance between the sound source and the reflector. Cumulatively, the gain is maximum when the reflector is 1m and minimum when the reflector is at 3.2 m away from the sound source over the range of frequencies.

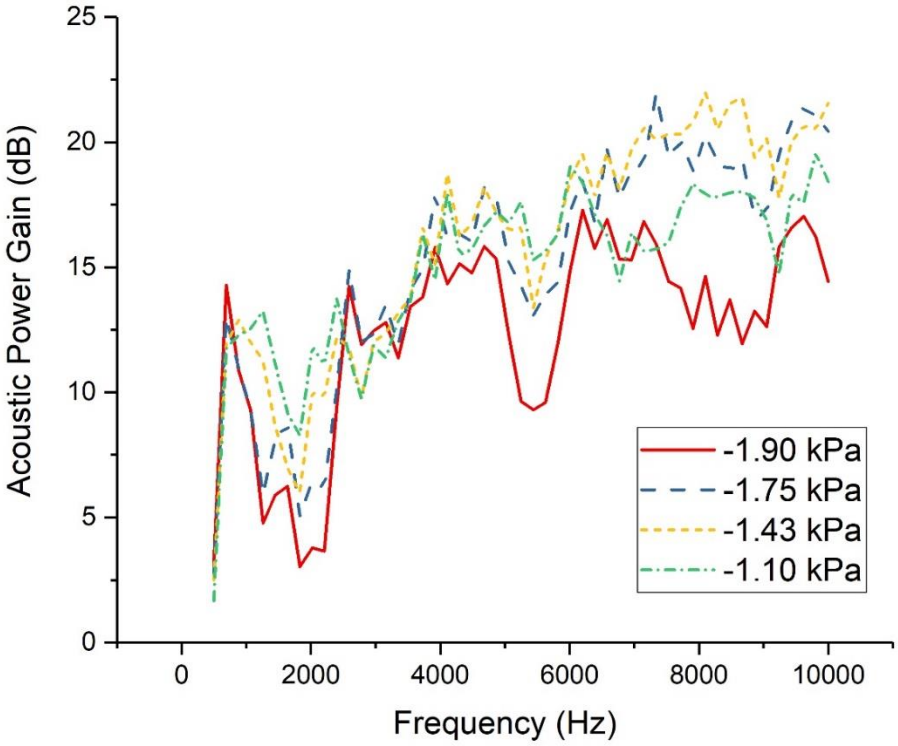

Figure 36: The plot indicates the variation of the plot for acoustic power gain against frequency where the microphone is fixed. The variation occurs due to change in the vacuum inside the reflector.

4.3 Acoustic Finite Element Analysis using COMSOL

We implemented the Acoustic-Shell interaction module within COMSOL. We considered a 3D module while performing simulations. The simulation comprised of 5 main domains; the speaker, aluminum reflector housing, Ecoflex reflecting surface, speaker, air domain and PMLs.

We modeled the body of the speaker as a cylinder with 0.1 m height and a diameter of 0.2 m. We modeled the diaphragm of the speaker as a cone with 0.1016 m top diameter, 0.02 m bottom diameter and 0.04 m as its height. The domain under consideration is twice the distance between the speaker and the acoustic reflector considered during experiments. We modeled the PMLs as layers to the air domain with a thickness equal to one third that of the wavelength under consideration. We considered the domain is comprising of linear elastic material. We modeled the body of the speaker using ABS plastic and the diaphragm using titanium.

In the simulation, we aligned the Reflector and the speaker axially considering the X-axis. Acoustic shell structure interaction Multiphysics couples pressure acoustics module as well the Shell module. We include the perfectly matched layers, the reflecting surface of the housing and the speaker within pressure acoustics. We modeled the speaker boundaries as shell elements with thickness 0.01m. We applied a pressure of 0.1 Pa on the diaphragm of the speaker.

We modeled the reflector housing boundaries as interior sound hard boundaries and imposed an interior impedance on the reflecting surface. The values of specific acoustic

impedance are from the data obtained by extrapolating the plots of the transfer function from the impedance tube experiment [7].

The focus of the parabola is:

$$x^2 = 4 * F(y - F) \qquad \textbf{(25)}$$

The expressions of the probe are “p” and “acpr.Lp” representing pressure and Sound Pressure Level.

We implemented a parametric sweep for the PML thickness, the frequency, specific impedance and mesh size. We exported the values obtained using simulation for 54 different frequencies and repeated the same without the parabolic reflector. The acoustic power gain is [12]:

$$Gain\ (dB) = 20 \log_{10} \frac{\text{Pressure with Reflector in Place}}{\text{Pressure without Reflector in Place}} \qquad \textbf{(26)}$$

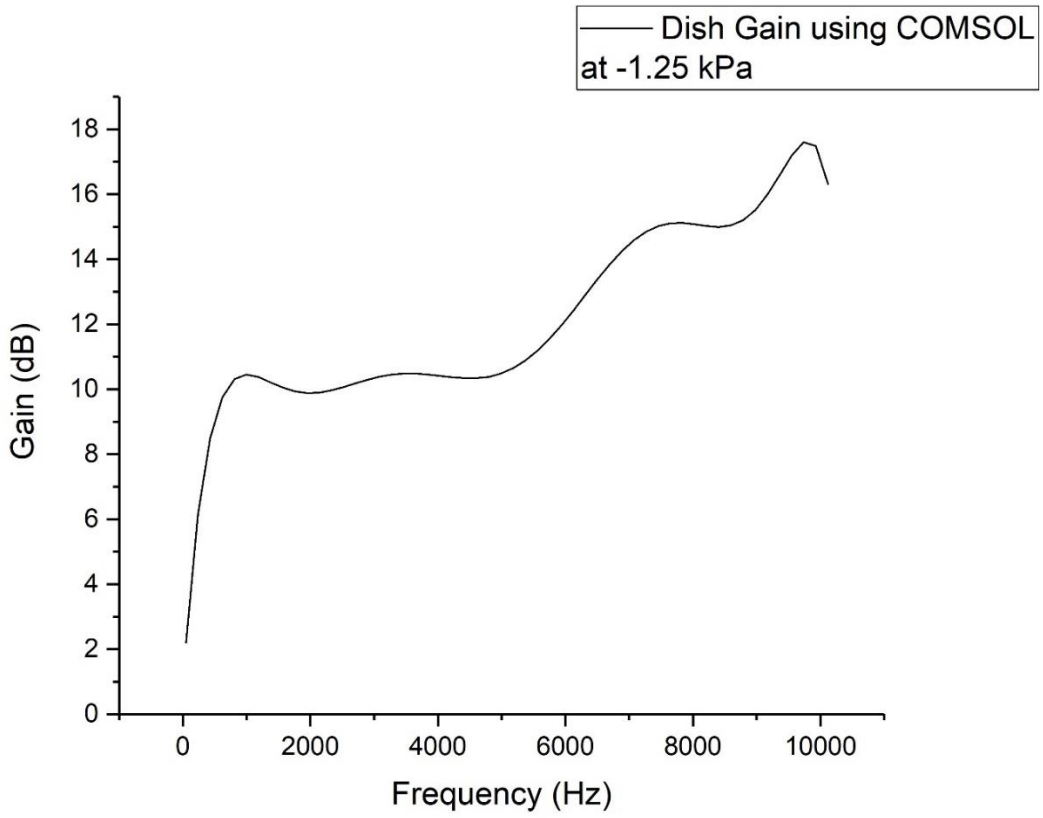

Figure 37: The above graph is a plot for the acoustic power gain obtained using COMSOL frequencies ranging from 50 Hz to 10120 Hz. We calculated the gain by recording the acoustic pressures for a range of frequencies, with and without the reflector in place.

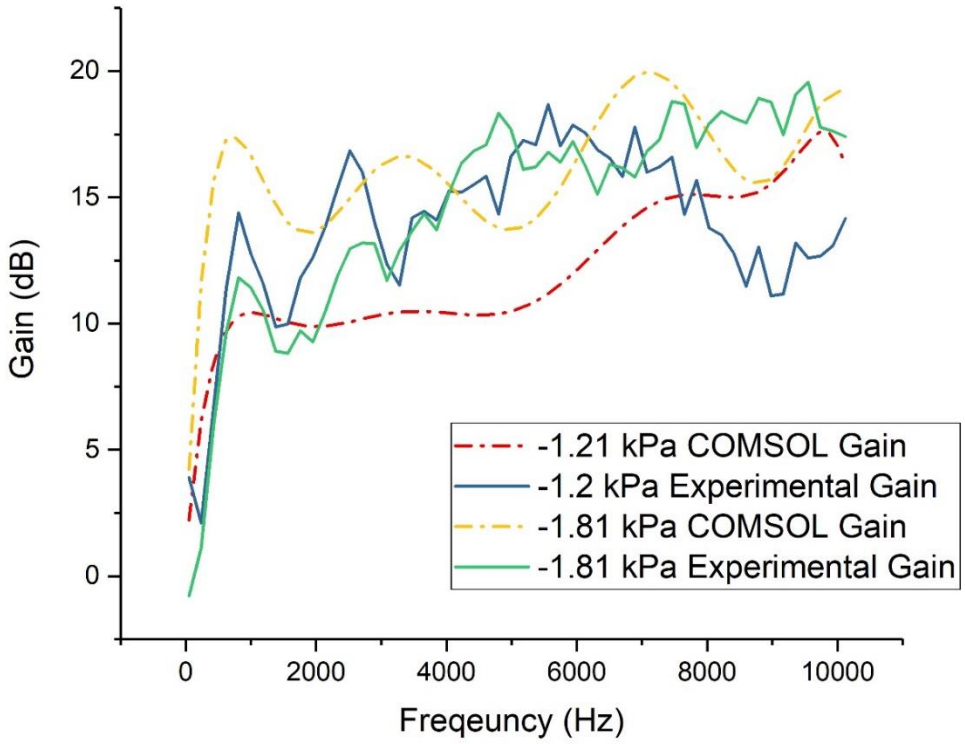

Figure 38: The above plot is a comparison of the nature of plots obtained experimentally to those obtained using COMSOL simulations for acoustic power gain.

4.4 Experimental Polar Response

We conducted on-axis testing to characterize the reflector for its directional response. The sound source was a Behringer Studio Monitor through which a sine wave of a set frequency and 0.1 V amplitude was output. We rotated the entire reflector microphone assembly using a NEMA 23 stepper motor. While conducting the directionality test, we started off-axis, from a point which is at a certain angle from the straight line joining the speaker and the speaker axis. This off-axis start ensured that we get two distinct peaks while conducting the entire test. The data received using the microphone was in the form of voltage. The two distinct peaks during rotation were detected using the max(); syntax in MATLAB. The two peaks detected the start and end indices of the time vector under consideration. We divided the data into 360 portions and fit sine waves per portion. We plot a Sound Pressure Level versus Time plot to see the nature of the filtered data. We made use of the amplitude of the fitted sine wave per portion to plot a polar plot which is the directional response of our parabolic microphone. We conducted the entire experiment for four distinct frequencies 1000, 4000, 7000 and 10,000 Hz. We controlled the rotation of the reflector assembly using G-codes and a feed rate of "1". The vacuum levels implemented were -1.79, -1.63 kPa, -1.5 kPa, -1.31 kPa, -1.29 kPa, -1.22 kPa. It takes 52 seconds for one complete revolution. We plot a normalized polar plot for these vacuum levels at 7000 Hz.

From the nature of the polar plots obtained we observe that the polar plot for 1000 Hz has the largest lobe on both the sides. The polar plot for 10,000 Hz has the smallest lobes and is tightly fit. From Figure 38, we also observe that the polar plots shrink in size for higher vacuum levels.

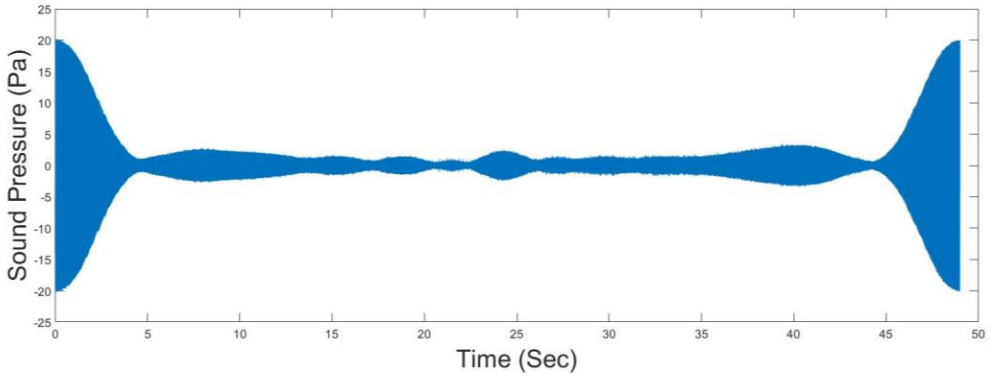

Figure 39: Sound Pressure Level vs Time plot obtained using MATLAB at 4000 Hz and a vacuum of -1.79 kPa where the sampling rate is 51200.

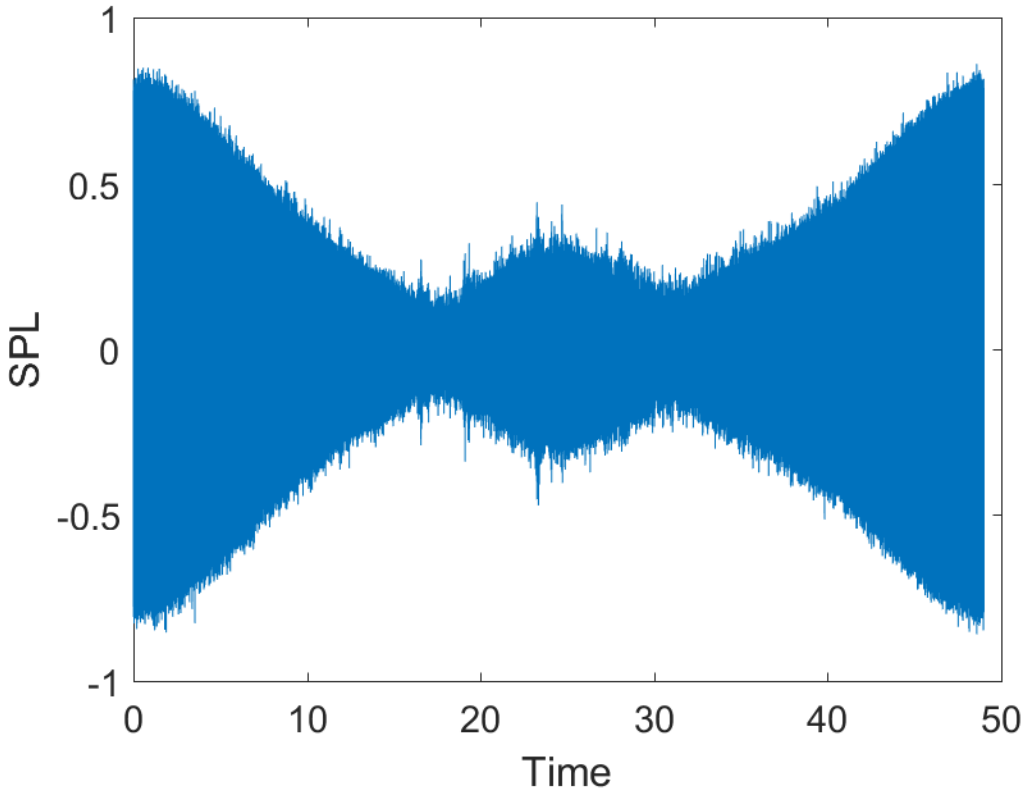

Figure 40: Sound Pressure Level Vs Time plot obtained using MATLAB for 1000 Hz and a vacuum of -1.79 kPa where the sampling rate is 51200.

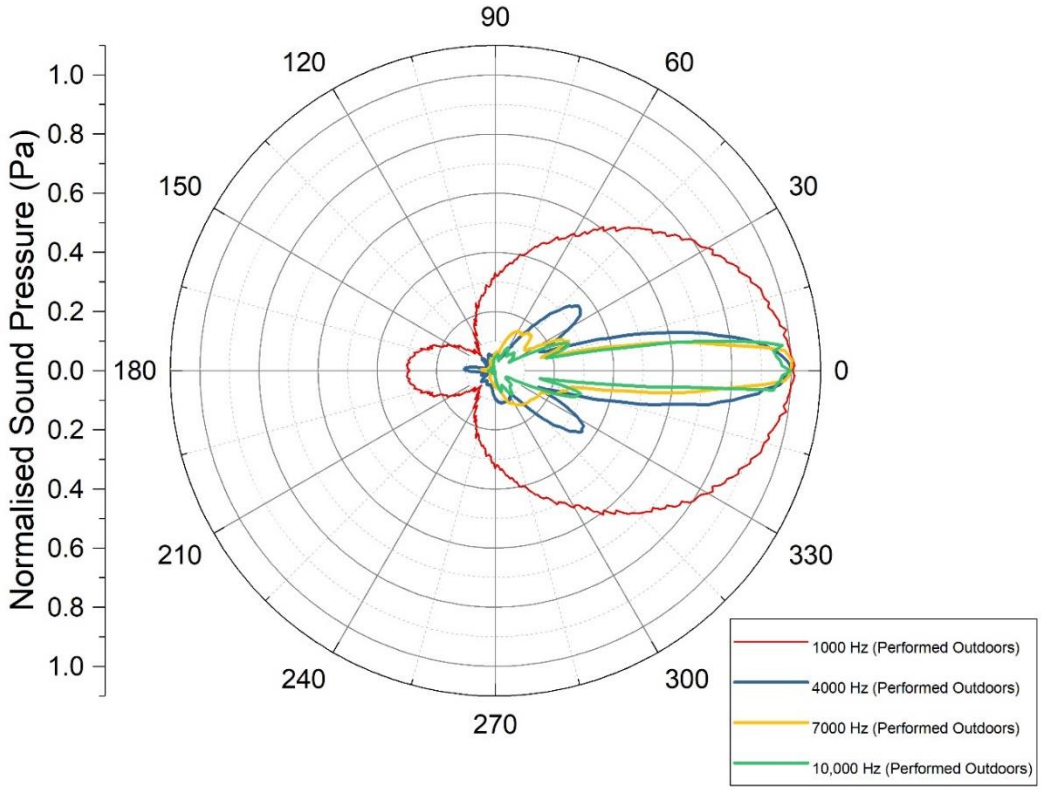

Figure 41: The normalized polar plot indicates the nature and distribution of polar plots obtained experimentally for a vacuum of -1.79kPa within the reflector and frequencies ranging between 1000 Hz and 10,000 Hz. The microphone is less directional for lower frequencies and the directional response increases for higher frequencies due to attenuation.

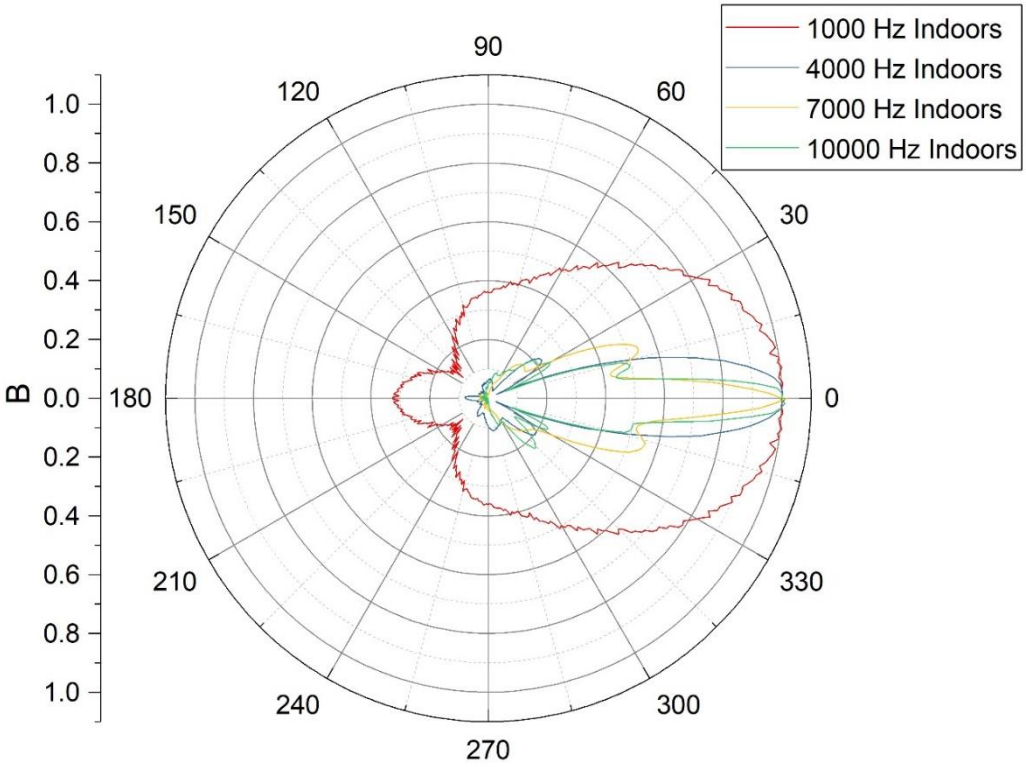

Figure 42*:* The normalized polar plot indicates the nature and distribution of polar plots obtained experimentally for a vacuum of -1.79kPa within the reflector and frequencies ranging between 1000 Hz and 10,000 Hz for an experiment performed indoors. The microphone is less directional for lower frequencies and the directional response increases for higher frequencies due to attenuation.

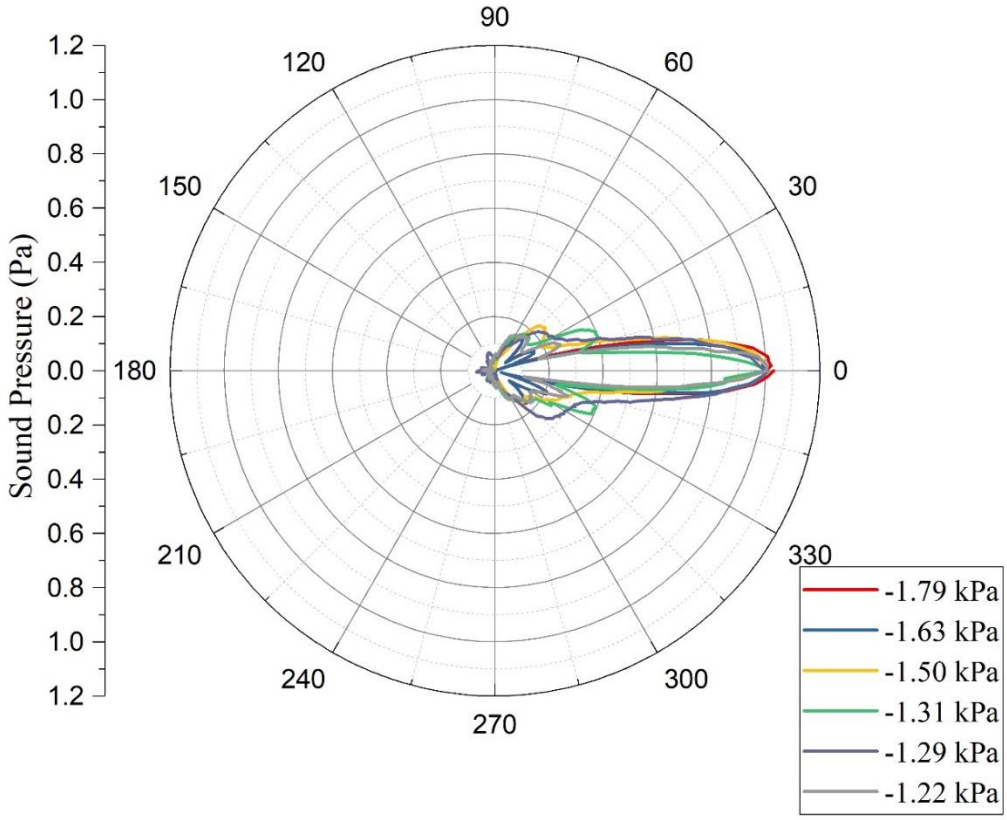

Figure 43: The plot represents the change in the polar plot observed for 7000 Hz. We swept through 6 different vacuum levels ranging from -1.79 kPa to -1.22 kPa. The variation of the polar plots observed is due to the modified focal length corresponding to a vacuum level. From the graph, we conclude that for -1.79 kPa the lobe in the region between 180 to 270 degrees is smaller as compared to -1.22 kPa. The dish microphone becomes more directional as the vacuum increases.

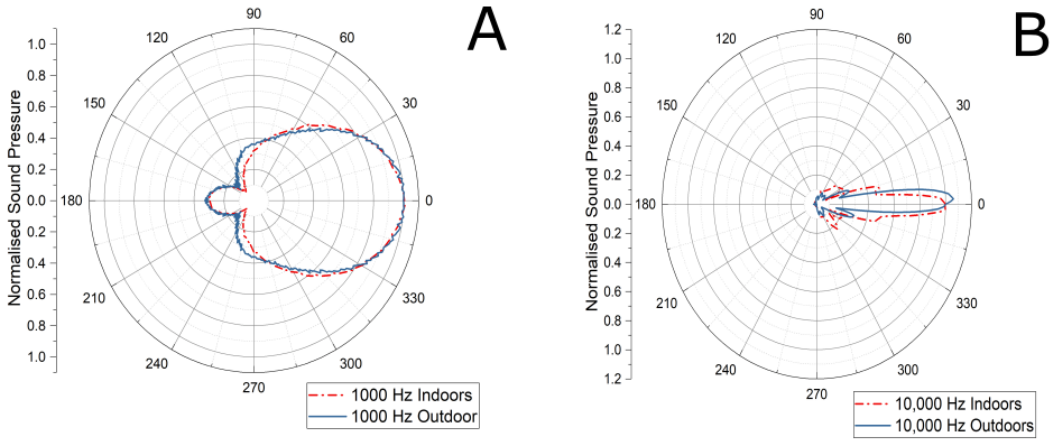

Figure 44: Figure A & B indicate an overlay of the experimental polar response for 1000 Hz and 10,000 Hz for experiments performed indoors and outdoors. The polar responses for experiments performed indoors appear more symmetrical about the neutral axis.

4.5 Directionality using Acoustic Finite Element Analysis implementing COMSOL

The directionality simulation also has three main components, the Acoustic Parabolic Reflector, the speaker modeled in the form of a cylinder and a spherical domain of diameter 2 m with PML layers to it. While performing simulations, we placed a probe at the focus of the parabola formed by the surface. We rotated the sound source about the reflector and recorded the pressure per degree rotation. We used the acoustic shell interaction submodule within the pressure acoustics module. We implemented a parameter “theta” for the rotation of the reflector about the focus of the microphone. For every intermediate theta, we recorded the magnitude of the pressure using a probe placed at the focus. We plot the normalized pressure vector per degree using a polar plot. We performed the simulation using a 3D domain. Figure 45,46 shows the focusing of incoming sound waves using the reflector and application of impedance boundary conditions.

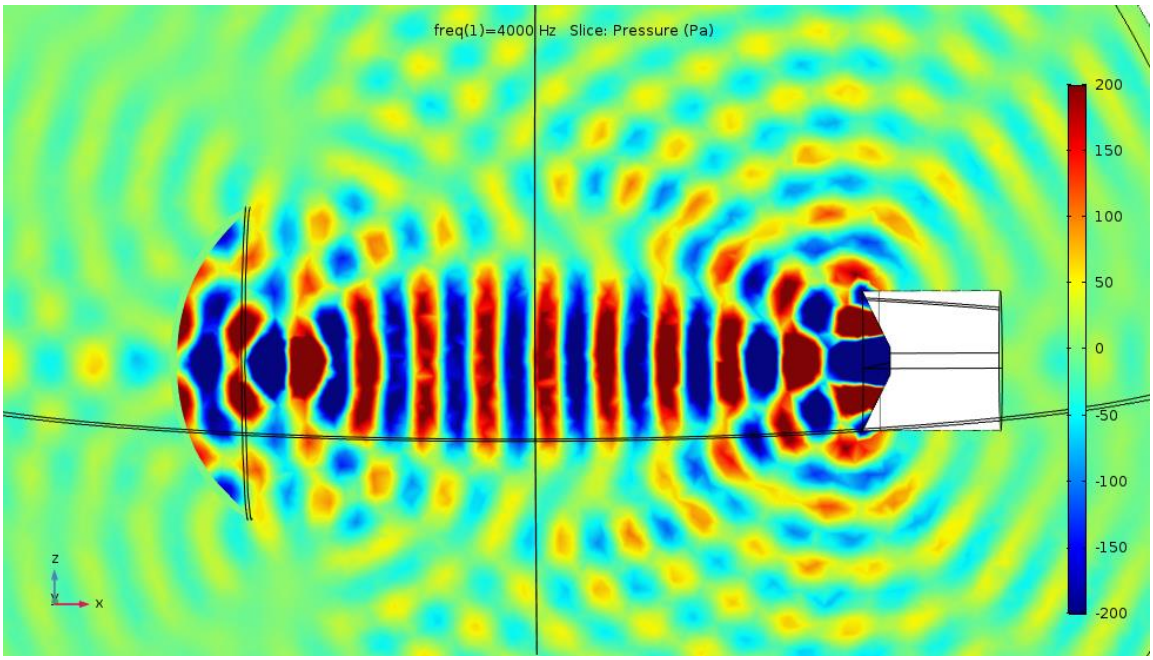

Figure 45: A 3D Acoustic Shell Structure Simulation to demonstrate the focusing of incident sound waves at 4000 Hz. We applied a pressure of 0.1 Pa on the diaphragm of the membrane. We kept the speaker and the parabolic reflector 1 m apart from each other.

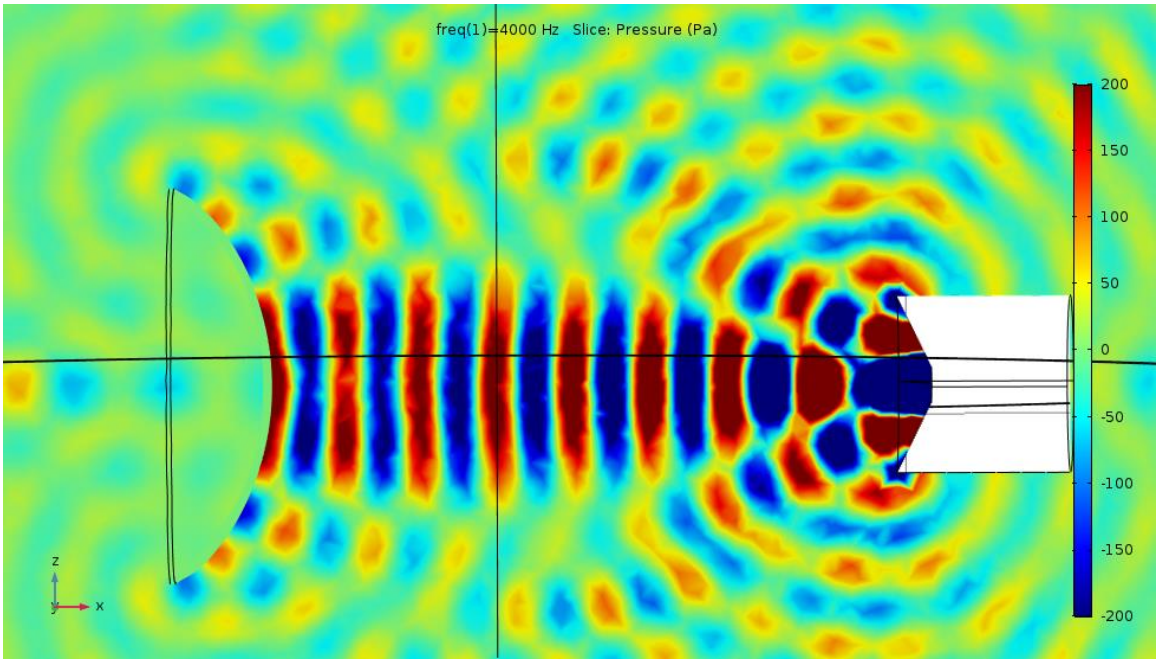

Figure 46: A 3D Acoustic Shell Structure Simulation to demonstrate the divergence of incident sound waves at 4000 Hz. We applied a pressure of 0.1 Pa on the diaphragm of the membrane. We kept the speaker and the parabolic reflector 1 m apart from each other.

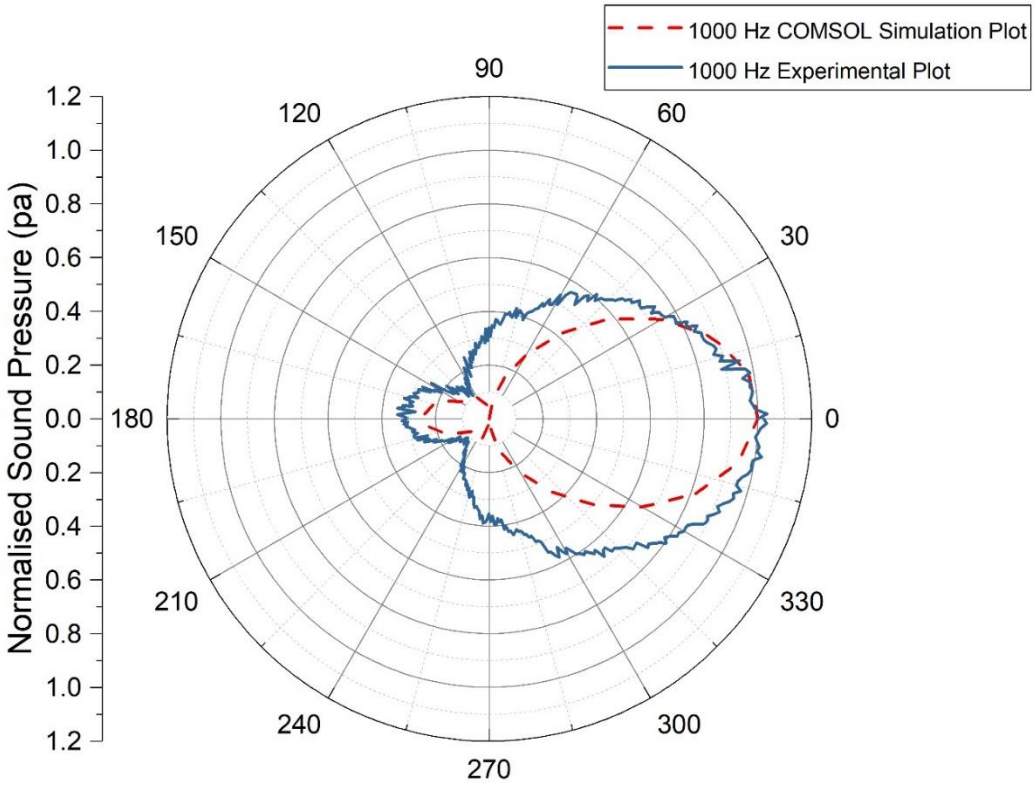

Figure 47: Normalized polar plot obtained experimentally and by using COMSOL simulation for 1000 Hz. The nature of polar plots obtained experimentally and that obtained using COMSOL agree qualitatively.

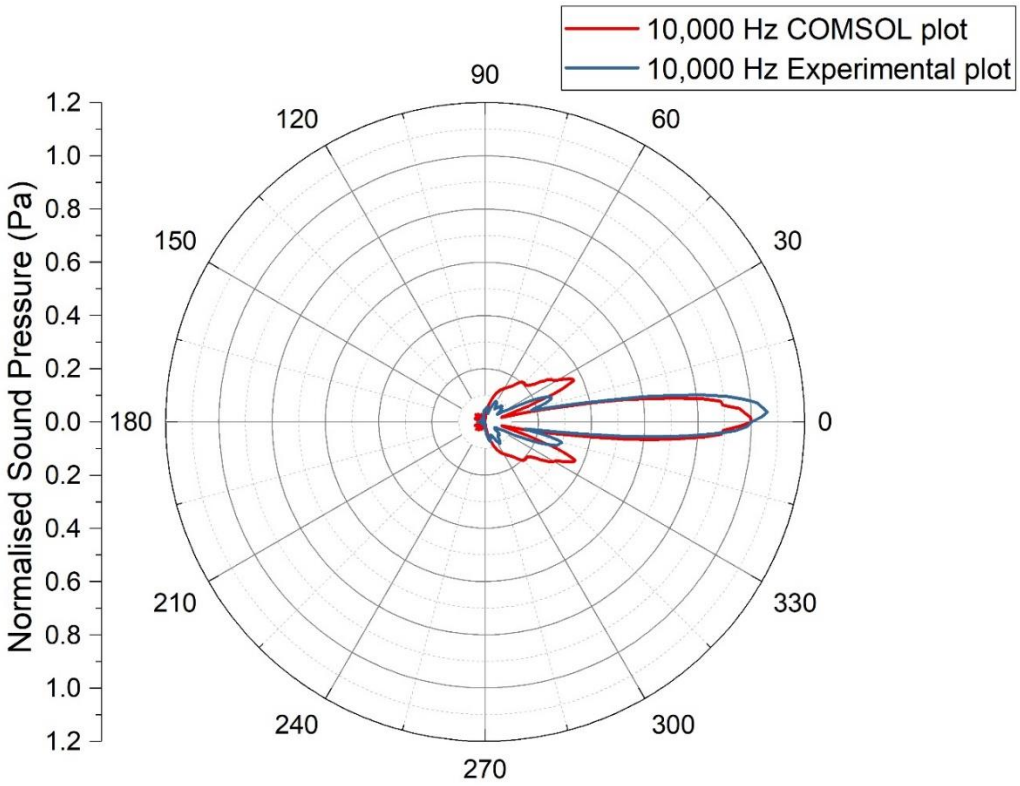

Figure 48: Figure: Normalized polar plot obtained experimentally and by using COMSOL simulation for 10000 Hz. The nature of polar plots obtained experimentally and that obtained using COMSOL agree qualitatively.

5. Conclusion

We designed the reflector housing structure and plumbing to measure vacuum for an air-tight reflector. We made the assembly vacuum tight using a method like that of a pre-stressed drum membrane. We achieved distinct vacuums by measuring the vacuum inside the reflector housing by implementing concise plumbing. We successfully performed the experiments outdoors.

The plot of the deformed profiles of the membrane obtained using COMSOL indicates the parabolic nature of the membrane when deformed by application of vacuum. We obtained a relationship between the radial displacement of the membrane and the deformation using a COMSOL plot.

The acoustic power gain demonstrates an increasing trend, for higher frequencies as the vacuum increases. Plot obtained using COMSOL for acoustic power gain agrees qualitatively with that obtained experimentally. The typical efficiency of the dish of a parabolic dish microphone is between 45% to 70% [2]. The efficiency of our parabolic dish is 42.61%. The small error may arise due to construction and assembly of the individual components. The maximum acoustic power gain recorded by the system experimentally is ~17 dB for frequencies ranging 7500 Hz to 8000 Hz. This gain is comparable to the gain obtained in the paper “Parabolic Dish Microphone Systems” by Robert Maher[2]. The nature of the plot obtained for Acoustic Power gain agrees with the plot in the paper “Reflector Microphones for Field Recording of Natural Sounds.”[14].

The directional response of our microphone is a Super hyper-cardioid which is similar to the parabolic microphones available commercially[15]. The size of the lobes varies per

frequency. The lobes observed for 1000 Hz were large as compared to 10,000 Hz. The microphone becomes less directional for higher frequencies observe greater loss with distance due to attenuation than at lower frequencies.

During our experiment, we applied a modest vacuum in the range 0 to -1.9 kPa. The microphone becomes more directional with increased vacuum due to higher focusing ability than at lower frequencies. While conducting experiments, we also considered the situation where we have a sound source placed axially beyond 1m and farthest at 3.2m from the reflector. The nature of the plot for Acoustic Power Gain (dB) Vs Frequency (Hz) has a decreasing trend when we move the sound source further apart from the speaker. Simulations performed using plane waves indicate the ability of the reflector to focus sound waves from a distant sound source.

We simulated an ideal case using COMSOL for gain and directionality. We considered a domain of diameter 2m and Perfectly Matched layers of thickness one-third that of the wavelength. The results obtained from these experiments have certain agreement with the experiments performed outdoors. We demonstrated the effect of uniformly stretching the membrane using COMSOL.

Since the aluminum reflector was over 1 kg and the mounting base was an aluminum C channel, the reflector assembly vibrated to a certain extent while revolving which induced stray noise. The model gets computationally expensive for higher frequencies as the degrees of freedom required to resolve waves over 5000 Hz is ~10^9.

We can implement a similar assembly method for a dish of larger diameter to enhance the gain of the parabolic microphone. Since it's feasible to experiment outdoors, we could use

the same apparatus to explore the effect of wind on the directionality and gain. In the future, we could integrate the reflectors in an array system to enhance the gain of the system.

6. References

[1] Paul Wade, “W1GHZ Microwave Antenna Book,” in *W1GHZ Microwave Antenna Book*, 1998th ed., .

[2] Z. C. Robert C. Maher, “Parabolic Dish Microphone System,” presented at the Birdstrike, 2005.

[3] Martijn Vercammen, “SOUND CONCENTRATION CAUSED BY CURVED SURFACES,” Technische universiteit eindhoven.

[4] Knowles Electronics, Inc., “Directional Microphone Applications.” 2017.

[5] H. L. R. Julianne Tjervåg Flø, “Parabolic Reflector for Focusing of Underwater Acoustic Waves,” The Arctic University of Norway, 2017.

[6] T. T. Ryoichi Takashima and Yasuo Ariki, “Evaluation of an Active Microphone with a Parabolic Reflection Board for Monaural Sound-Source-Direction Estimation,” in *Soundscape Semiotics - Localization and Categorization*, .

[7] Yanjun Wang, “ACOUSTIC MANIPULATION OF SOUND WITH SOFT MATERIAL-BASED ACTUATORS,” Rutgers University, 2015.

[8] James M. Gere, *Mechanics of Materials*, Sixth Edition. Thomson Learning, Inc.

[9] COMSOL Multiphysics, *Structural Mechanics Module User’s Guide COMSOL 5.3*, 5.3a. 2017.

[10] COMSOL Multiphysics, *Acoustic Module User’s Guide*, 5.3a. .

[11] “Standard Test Method for Impedance and Absorption of Acoustical Materials Using A Tube, Two Microphones and A Digital Frequency Analysis System1.” ASTM.

[12] Ethem Mutlu Sözer, “Underwater Acoustics A Brief Introduction.” .

[13] “Multi-field Microphone Type 4961 1/4’’ Microphone with TEDS.” Brüel & Kjær.

[14] George W. Swenson, Jr., “Reflector Microphones for Field Recording of Natural Sounds,” Construction Engineering Research Laboratories, 19980317072.

[15] Wildtronics, LLC, “Wildtronics Parabolic Microphone.” Wildtronics, LLC, Aug-2017.

7. Supporting Information and MATLAB Codes

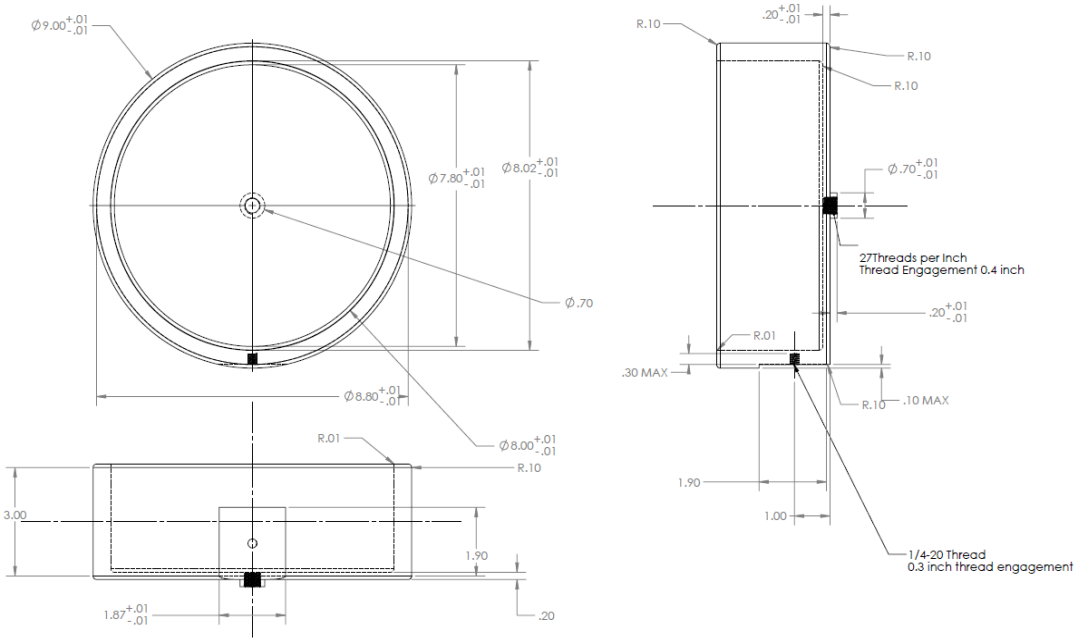

Figure 49: Machine Drawing for the Aluminum Reflector housing (units: inch)

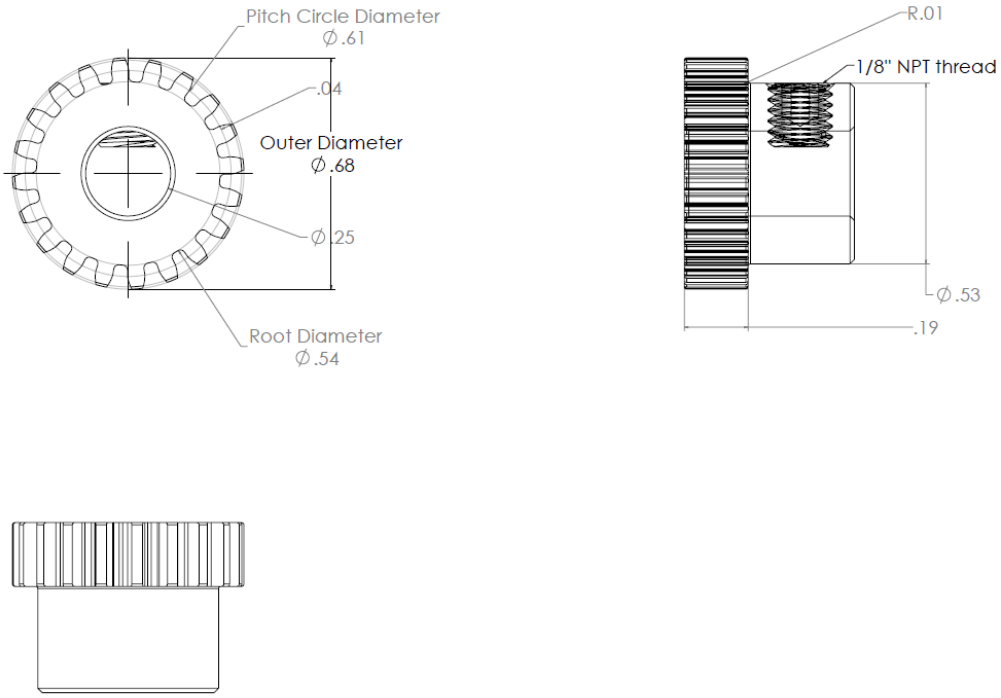

Figure 50: The gear mounted on the stepper motor which aids the rotation of the driven spur gear fixed to the reflector microphone assembly. (units: inch)

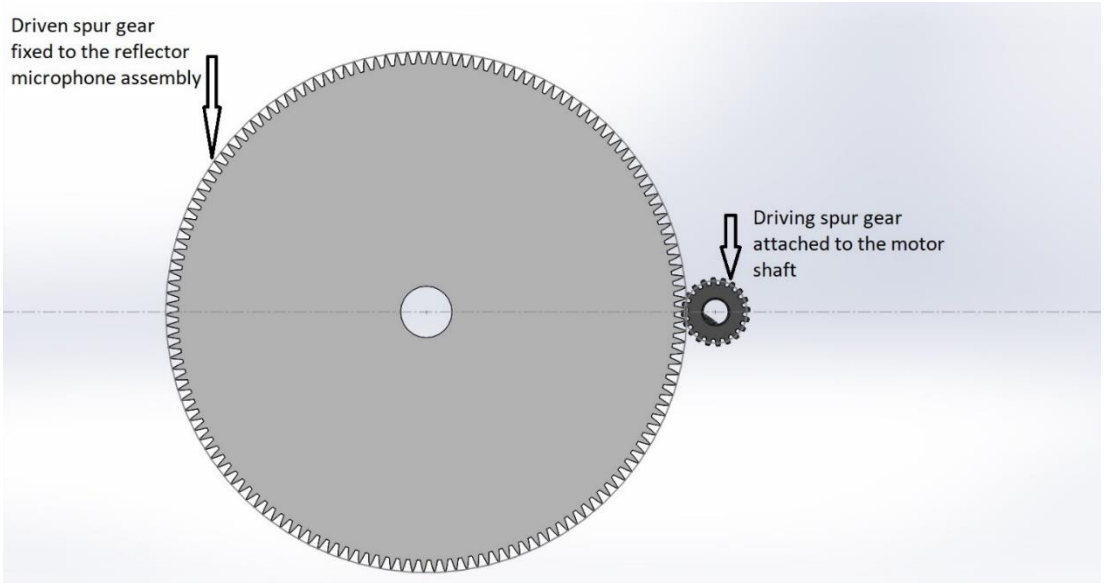

Figure 51: Meshing of the Spur gear attached to the reflector microphone assembly and the pinion attached to the stepper motor shaft.

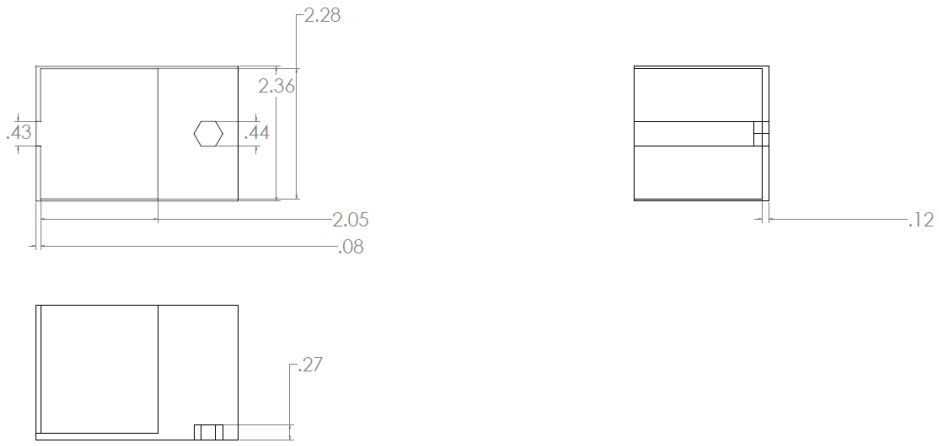

Figure 52: Mount to support the NEMA 23 stepper motor in the assembly (units: inch)

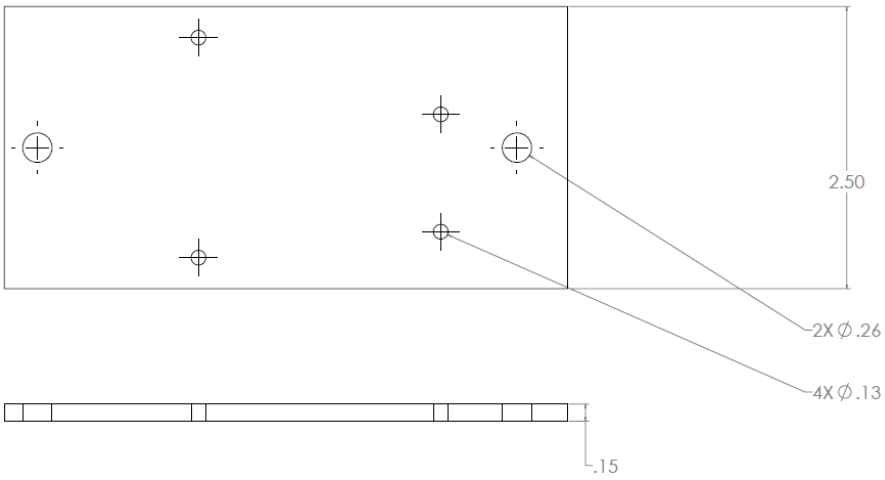

Figure 53: Mount to support the Arduino Uno board and the CNC shield (units: inch)

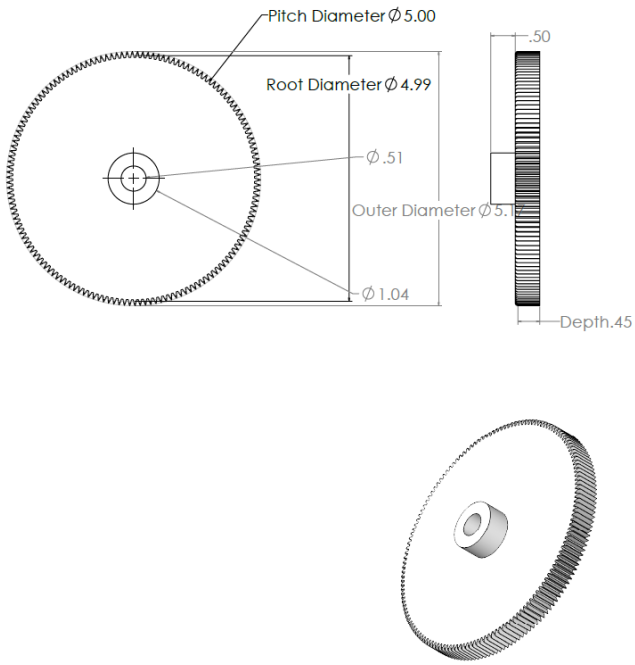

Figure 54: CAD drawing for the driven gear attached to the reflector microphone assembly using a press-fit (units: inch)

7. Acoustic Power Gain by implementing Highpass filter:

```
clc
clear all
close all
%% calculate focal length
diam = 8*2.54;
depthfrombarinch = 2.061;    % measure this
barthickness = 0.062;
% barthickness = 0;
focallength = diam^2/(16*(depthfrombarinch-barthickness)*2.54);
distance_between_bar_and_mic = focallength - depthfrombarinch*2.54;  %
in cm
positionofreflector = 1.8;
positionofmic = positionofreflector + 5.5 + (3.034 + barthickness)*2.54
+ distance_between_bar_and_mic

%% setup ni device
devices = daq.getDevices
% devices(1)

s = daq.createSession('ni');
% add microphone
addAnalogInputChannel(s,'cDAQ9184-1856596Mod1',0,'Microphone'); % 0
means we use the first connector of input card
% add wave generator
addAnalogOutputChannel(s,'cDAQ9184-1856596Mod2',1,'Voltage') % 1 means
we use the second group of connectors of input card (2 and 3)
% set the sensitivity of microphone
s.Channels(1).Sensitivity = 0.0582598; % channels(1) means the first
device we added

%% setup parameters
start_freq = 50 %start frequency
end_freq = 10120 %end frequency
step_freq = 190 %step frequency
s.Rate = 51200 %divide 1 second to s.Rate pieces (51200 is maximum
pieces we can divide)

loop_num = (end_freq - start_freq + step_freq)/ step_freq %calculate
the number of sweep
data=zeros(loop_num+1,s.Rate); % define a matrix for saving data
(loop_num: rows of data and 1: row of white noise)

%% record background noise and save it in row 1
loop_now = 1;

freq=1;
cycle=1;
amplitude=0;
output_data = amplitude*linspace(0,1,s.Rate)';

    for i=1:1:cycle
    queueOutputData(s,output_data);
    end
```

```
% plot(output_data);

duration = s.DurationInSeconds;

[data(loop_now,:),time] = s.startForeground();
loop_now = loop_now + 1;

% calibrate 0.1 V for amplifier

amp_cali = zeros(1,56)+0.5;
a_index = 1;
%% record each loop for each exciatation frequency
for f=start_freq:step_freq:end_freq
freq=f %define the frequency of output voltage
cycle=1; %define the number of second of output
amplitude=amp_cali(a_index) %define the amplitude of output 0.1V
a_index = a_index + 1;
% separate many sin waves into s.Rate pieces, the number of the sin
waves is the excitation frequency
output_data = amplitude*sin(linspace(0,freq*2*pi,s.Rate)'); %generate
output in one second

%generate output queue in a few of cycles(seconds)
    for i=1:1:cycle
    queueOutputData(s,output_data);% put them into 1 second
    end

% plot(output_data);

duration = s.DurationInSeconds; %calculate the time of output


[data(loop_now,:),time] = s.startForeground(); %start voltage generator
and microphone at the same time
loop_now = loop_now + 1;
end

%% save the data for data analysis in 'data_process.m' file
save(['1.0111162017WithoutReflector.mat'],'time','data');

 clc
clear all
close all
%% Highpass Filter
Fs = 51200;  % Sampling Frequency

Fstop = 5;              % Stopband Frequency
Fpass = 50;              % Passband Frequency
Dstop = 0.0001;          % Stopband Attenuation
Dpass = 0.057501127785;  % Passband Ripple
dens  = 20;              % Density Factor

% Calculate the order from the parameters using FIRPMORD.
```

```
[N, Fo, Ao, W] = firpmord([Fstop, Fpass]/(Fs/2), [0 1], [Dstop,
Dpass]);

% Calculate the coefficients using the FIRPM function.
b  = firpm(N, Fo, Ao, W, {dens});
Hd = dsp.FIRFilter( ...
    'Numerator', b);
%% load the data from the saved data for concave configuration
load('1.9111162017WithReflector.mat');
counter = 1;

% ttt = time;
% clear time;
for j=1:55
    data(j,:) = filter(b,1,data(j,:));
    for i=1:(51200/2)
        captured_data(j,i) = data(j,i + 51200/2);
%         captured_data(j,i + 51200/4) = data(j,i + 51200/2);
        captured_data(j,i + 51200/2) = 0;
%         captured_data(j,i + 51200*3/4) = data(j,i + 51200/2);
    end
    if (Fpass<1000 && counter>2)
        Fstop = Fstop + 170;
        Fpass = Fpass + 190;
        [N, Fo, Ao, W] = firpmord([Fstop, Fpass]/(Fs/2), [0 1], [Dstop,
Dpass]);
        b  = firpm(N, Fo, Ao, W, {dens});
    end
    counter = counter + 1;
end



%% Setup
start_freq = 50;
end_freq =10120;
step_freq = 190;

% For corpping data
t_estimate = 0;                     % estimate length of the pause
before the first frequency
fs = 51200;
% Estimated noise bed level
noise_bed = 0.09;
SNR_estimate = 2;
% Signal pattern
fq_number = 1;                                                  % number
of fq swept
fq_list = (linspace(50,10120,54))';
fq_duration = 0.75;                                               %
duration of each fq
pause_duration = 0;                                             % pause
duartion after each fq
number_delay = 0.5;                                               %
delay for locating the first peak
```

```
test_duration = fq_number*(fq_duration+pause_duration);          %
signal + pause after each fq
% Fitting
fq_delay = 0;                                                  % delay at
the beginning of each fq
num_wave = 45;                      % number of waveform taking into
curve fitting for each fq
n_fitted_ch1 = [];
% n_fitted_ch2 = [];
c_fitted_ch1 = [];
% c_fitted_ch2 = [];
% FFT plot window width
fft_ww = 0.4;
loop_now = 1;

%% main loop
for f = 1:1:(end_freq-start_freq)/step_freq+1

% Fetch neutral data
loop_now = loop_now + 1;
time_neutral = time(:,1);
data_neutral_ch1 = captured_data(loop_now,:);


%% Corp Data (Concave)

% Grab Ch1 and find peaks
peak_sig_neutral = data_neutral_ch1;
[pks_neutral,locs_neutral] = findpeaks(peak_sig_neutral);
% Corp data
n_ch1 = data_neutral_ch1';
% n_ch2 = data_neutral_ch2(starting_point_neutral:end_point_neutral,1);
sz_neutral = size(n_ch1(:,1));                                 % Zero
time
n_time = time_neutral;
% Plot time domain
figure
plot(n_time,n_ch1);
title('Time Domain (Concave)','FontSize',16);
xlabel('Time (s)','FontSize',16);
ylabel('Pressure (pa)','FontSize',16);
set(gca,'FontSize',14);
% saveas(gcf,'concave_time_domain.png');

%% Curve Fitting (Concave)
fq_count=1;
step=(fq_duration+pause_duration)*fs;
fq_start_pt=step*fq_count;
i = loop_now-1;

    % locate 10 waveform
    n_start_pt=round(1);              % pick starting point for each fq
    n_end_pt=n_start_pt+num_wave/fq_list(i)*fs;      % take 100
waveform out for each fq
    % fetch data
```

```
    X = n_time(round(n_start_pt):round(n_end_pt),1);
    Y1 = n_ch1(round(n_start_pt):round(n_end_pt),1);
    if f==1
    Y1(25601:46081)=Y1(1:20481);
    end
%]     Y2 = n_ch2(n_start_pt:n_end_pt,1);
    Y0 = n_ch1(1:fq_duration*fs,1);
    time_start = n_time(round(n_start_pt));
    time_end = n_time(round(n_end_pt));
    x = linspace(time_start,time_end,1000000);

    % curve fitting

    fo = fitoptions('Method','NonlinearLeastSquares');
    ft = fittype(' a1*sin(b1*x+c1)','problem','b1','options',fo);
    [fn_ch1.fit,fn_ch1.G] = fit(X,Y1,ft,'problem',fq_list(i)*2*pi);
%     [fn_ch2.fit,fn_ch2.G] = fit(X,Y2,ft,'problem',fq_list(i)*2*pi);
    n_fitted_ch1 = [n_fitted_ch1;abs(fn_ch1.fit.a1)];
% save the amplitude of the fitted sine wave
%     n_fitted_ch2 = [n_fitted_ch2;abs(fn_ch2.fit.a1)];


    figure
    subplot(2,1,1);

plot(X,Y1,'.b',x,fn_ch1.fit.a1*sin(fn_ch1.fit.b1.*x+fn_ch1.fit.c1),'r',
'MarkerSize',14,'LineWidth',2);
    title([num2str(fn_ch1.fit.b1/2/pi,'%.0f'),' Hz concave
Ch1'],'FontSize',16);
    xlim([time_start time_end]);
    grid on;
    set(gca,'FontSize',14);



    % FFT for Ch1
    L1 = length(Y0);
    NFFT = 2^nextpow2(L1); % Next power of 2 from length of y
    Y0_fft = fft(Y0,NFFT)/L1;
    f0 = fs/2*linspace(0,1,NFFT/2+1);
    abs_Y0=2*abs(Y0_fft(1:NFFT/2+1));


    subplot(2,1,2);
    plot(f0,abs_Y0,'MarkerSize',14,'LineWidth',2)
    title('Amplitude Spectrum Ch1','FontSize',16)
    xlabel('Frequency (Hz)','FontSize',14)
    ylabel('|Y(f)|','FontSize',14)
    xlim([(1-fft_ww)*fq_list(i) (1+fft_ww)*fq_list(i)]);
    grid on;
    set(gca,'FontSize',14);

    saveas(gcf,['concave_',num2str(fq_list(i),'%.0f'),' Hz.png']);
    close all;
```

```
end
c_fitted_ch1 = n_fitted_ch1;        %save amplitudes to concave
variable
clear n_fitted_ch1;
n_fitted_ch1 = [];

%% load the data from the saved data for neutral configuration
load('1.83WithoutReflrctorOpenAir.mat');
counter = 1;

% ttt = time;
% clear time;
for j=1:55
    data(j,:) = filter(b,1,data(j,:));
    for i=1:(51200/2)
        captured_data(j,i) = data(j,i + 51200/2);
%         captured_data(j,i + 51200/4) = data(j,i + 51200/2);
        captured_data(j,i + 51200/2) = 0;
%         captured_data(j,i + 51200*3/4) = data(j,i + 51200/2);
    end
    if (Fpass<1000 && counter>2)
        Fstop = Fstop + 170;
        Fpass = Fpass + 190;
        [N, Fo, Ao, W] = firpmord([Fstop, Fpass]/(Fs/2), [0 1], [Dstop,
Dpass]);
        b  = firpm(N, Fo, Ao, W, {dens});
    end
    counter = counter + 1;
end

loop_now = 1;
%% main loop
for f = 1:1:(end_freq-start_freq)/step_freq+1

% Fetch neutral data
loop_now = loop_now + 1;
time_neutral = time(:,1);
data_neutral_ch1 = captured_data(loop_now,:);
% data_neutral_ch2 = data(:,2);

%% Corp Data (Neutral)

% Grab Ch1 and find peaks
peak_sig_neutral = data_neutral_ch1;
[pks_neutral,locs_neutral] = findpeaks(peak_sig_neutral);

n_ch1 = data_neutral_ch1';
% n_ch2 = data_neutral_ch2(starting_point_neutral:end_point_neutral,1);
sz_neutral = size(n_ch1(:,1));                                  % Zero
time
n_time = time_neutral;
% Plot time domain
figure
```

```
plot(n_time,n_ch1);
title('Time Domain (Neutral)','FontSize',16);
xlabel('Time (s)','FontSize',16);
ylabel('Pressure (pa)','FontSize',16);
set(gca,'FontSize',14);
% saveas(gcf,'neutral_time_domain.png');

%% Curve Fitting (Neutral)
fq_count=1;
step=(fq_duration+pause_duration)*fs;
fq_start_pt=step*fq_count;
i = loop_now-1;

    % locate 10 waveform
    n_start_pt=round(1);              % pick starting point for each fq
    n_end_pt=n_start_pt+num_wave/fq_list(i)*fs;      % take 100
waveform out for each fq
    % fetch data
    X = n_time(round(n_start_pt):round(n_end_pt),1);
    Y1 = n_ch1(round(n_start_pt):round(n_end_pt),1);
    if f==1
    Y1(25601:46081)=Y1(1:20481);
    end
%     Y2 = n_ch2(n_start_pt:n_end_pt,1);
    Y0 = n_ch1(1:fq_duration*fs,1);
    time_start = n_time(round(n_start_pt));
    time_end = n_time(round(n_end_pt));
    x = linspace(time_start,time_end,1000000);

    % curve fitting

    fo = fitoptions('Method','NonlinearLeastSquares');
    ft = fittype(' a1*sin(b1*x+c1)','problem','b1','options',fo);
    [fn_ch1.fit,fn_ch1.G] = fit(X,Y1,ft,'problem',fq_list(i)*2*pi);
%     [fn_ch2.fit,fn_ch2.G] = fit(X,Y2,ft,'problem',fq_list(i)*2*pi);
if (f<7)
    n_fitted_ch1 = [n_fitted_ch1;abs(fn_ch1.fit.a1)];
else
    n_fitted_ch1 = [n_fitted_ch1;abs(fn_ch1.fit.a1)];
end% save the amplitude of the fitted sine wave
%     n_fitted_ch2 = [n_fitted_ch2;abs(fn_ch2.fit.a1)];
    figure
    subplot(2,1,1);
    if (f<7)

plot(X,Y1,'.b',x,fn_ch1.fit.a1*sin(fn_ch1.fit.b1.*x+fn_ch1.fit.c1),'r',
'MarkerSize',14,'LineWidth',2);
    title([num2str(fn_ch1.fit.b1/2/pi,'%.0f'),' Hz neutral
Ch1'],'FontSize',16);
    xlim([time_start time_end]);
    grid on;
    set(gca,'FontSize',14);
    else

plot(X,Y1,'.b',x,fn_ch1.fit.a1*sin(fn_ch1.fit.b1.*x+fn_ch1.fit.c1),'r',
'MarkerSize',14,'LineWidth',2);
```

```
    title([num2str(fn_ch1.fit.b1/2/pi,'%.0f'),' Hz neutral
Ch1'],'FontSize',16);
    xlim([time_start time_end]);
    grid on;
    set(gca,'FontSize',14);
    end



    % FFT for Ch1
    L1 = length(Y0);
    NFFT = 2^nextpow2(L1); % Next power of 2 from length of y
    Y0_fft = fft(Y0,NFFT)/L1;
    f0 = fs/2*linspace(0,1,NFFT/2+1);
    abs_Y0=2*abs(Y0_fft(1:NFFT/2+1));


    subplot(2,1,2);
    plot(f0,abs_Y0,'MarkerSize',14,'LineWidth',2)
    title('Amplitude Spectrum Ch1','FontSize',16)
    xlabel('Frequency (Hz)','FontSize',14)
    ylabel('|Y(f)|','FontSize',14)
    xlim([(1-fft_ww)*fq_list(i) (1+fft_ww)*fq_list(i)]);
    grid on;
    set(gca,'FontSize',14);

    saveas(gcf,['neutral_',num2str(fq_list(i),'%.0f'),' Hz.png']);
    close all;



%% plot theoretical vs experimental gain
fq_number = 54;
fq_list = (linspace(50,10120,fq_number))';

figure
color_num = linspace(1,1500,5);
dish_gain = 20.*log10(c_fitted_ch1./n_fitted_ch1);
plot(fq_list,dish_gain,'--*','MarkerSize',10,'LineWidth',1);
xlabel('Frequency (Hz)','FontSize',28);
ylabel('Gain (dB)','FontSize',28);
grid on;
set(gca,'FontSize',20);
hold on

% figure
% subplot(2,1,1)
% plot(343.3./fq_list,c_fitted_ch1)
% subplot(2,1,2)
% plot(343.3./fq_list,n_fitted_ch1)
%%
ff = linspace(1900,10100,50);
G1 = [];
d2 = 0.1;
G2 = 0.4*(d2*pi/343)^2.*ff.^2;
```

```
GdB2 = 10.*log10(G2);
xlim([1900 10100]);
plot(ff,GdB2,'LineWidth',3);
legend('Experimental','Theoretical','Location','SE','Orientation','hori
zontal','FontSize',28)
print('gain_40in', '-dpng', '-r600'); %Save as PNG with 600 DPI
```

Experimental Directionality:

```
% clc
% clear all
% close all
%% calculate focal length
diam = 14;
depthfrombarinch = 1.291;   % measure this
focallength = diam^2/(16*(depthfrombarinch-0.412)*2.54);
distance_between_bar_and_mic = focallength - depthfrombarinch*2.54
%% setup ni device
devices = daq.getDevices
tic
devices(1)
% d=serial('COM3');
% d.baudrate=115200;
% fopen(d);
s = daq.createSession('ni');
% add microphone
addAnalogInputChannel(s,'cDAQ9184-1856596Mod1',0,'Microphone'); % 0
means we use the first connector of input card
% add wave generator
addAnalogOutputChannel(s,'cDAQ9184-1856596Mod2',1,'Voltage') % 1 means
we use
s.Rate = 44100 %divide 1 second to s.Rate pieces (51200 is maximum
pieces we

%% record tone and save it
loop_now = 1;

freq=4000;          % Edit this
cycle=1;
amplitude=0.1;
duration = 50;      % in seconds
% s.DurationInSeconds = 50;
% s.ScansQueued = s.ScansQueued*20;
output_data =
amplitude*sin(linspace(0,freq*2*pi*duration,s.Rate*duration)');
%generate output in one second

%     for i=1:1:cycle

    queueOutputData(s,Q(:,1));
%     end

% plot(output_data);
```

```
% duration = s.DurationInSeconds;
% fprintf(d,'g03f3z50')
[data(loop_now,:),time] = s.startForeground();
loop_now = loop_now + 1;

% calibrate 0.1 V for amplifier

amp_cali = zeros(1,53)+1;
a_index = 1;
data = data;
save(['CheckMaryHadaLittleLamb3.mat'],'time','data');
toc

%% calculate focal length
diam = 14;
depthfrombarinch = 1.062;   % measure this
focallength = diam^2/(16*(depthfrombarinch-0.412)*2.54);
distance_between_bar_and_mic = focallength - depthfrombarinch*2.54

clc;
clear all;
close all;
tic
%% setup
srate = 51200;
num_step = 360;
n = 30;   % how many wavelength being taken to curve fitting

%% Concave

% training
load('1.65noReflector.mat');
filename = 'training';
fq = 10000;
time_start = 11;
time_end = 60;

firstdelay = 7;  % approximately how many secclear alonds until dish
rotates to directly face speaker
duration = 50;  % approximate duration for dish to return to facing
forward position
buffer = 8;

count = 1;
for i=(51200*firstdelay:51200*(firstdelay + duration/2))
    firstpart(i) = data(i);
    count = count + 1;
end

count = 1;
for i=(51200*(firstdelay + duration/2 + buffer):51200*(firstdelay +
duration + buffer))
    secondpart(i) = data(i);
    count = count + 1;
end
```

```
[firstpeak,p1] = max(firstpart);
[secondpeak,p2] = max(secondpart);

time_start = time(p1);
time_end = time(p2);
% edit time_start and time_end to make the graph better
   time_start = 11;
   time_end = 20;

data = data';

%% Highpass Filter
Fs = 51200;  % Sampling Frequency

Fstop = 300;              % Stopband Frequency
Fpass = 400;              % Passband Frequency
Dstop = 0.0001;           % Stopband Attenuation
Dpass = 0.057501127785;   % Passband Ripple
dens  = 20;               % Density Factor

% Calculate the order from the parameters using FIRPMORD.
[N, Fo, Ao, W] = firpmord([Fstop, Fpass]/(Fs/2), [0 1], [Dstop,
Dpass]);

% Calculate the coefficients using the FIRPM function.
b  = firpm(N, Fo, Ao, W, {dens});
Hd = dsp.FIRFilter( ...
    'Numerator', b);

data = filter(b,1,data);

%% corp data %% Updated data for SPL plot
pt_start = round(time_start*srate);
pt_end = round(time_end*srate);
data_cycle(:,1) = data(pt_start:pt_end,1);
% data_cycle(:,1)=data_cycle(:,1)/0.0523;
%% corp and zero time
sz = size(data_cycle(:,1));
time_cycle(:,1) = time(pt_start:pt_end,1);
time_cycle_zeroed(:,1) = time_cycle(:,1)-time_cycle(1)*ones(sz);

figure
plot(time_cycle_zeroed(:,1),data_cycle(:,1));
xlabel('Time','FontSize',14);
ylabel('SPL','FontSize',14);
set(gca,'FontSize',14);
saveas(gcf,['time domain',filename,' .png']);

%% curve fittng
i = linspace(0,(num_step-1),num_step);
[d1,d2] = size(data_cycle(:,1));
step = d1/num_step;
time_step = step*i;
fitted_ch1 = [];
```

```
for i=1:num_step
    fit_startpt = round(time_step(i)+1);
    fit_endpt = round(fit_startpt+n/fq*srate);
    X = time_cycle_zeroed(fit_startpt:fit_endpt,1);
    Y = data_cycle(fit_startpt:fit_endpt,1);
    x =
linspace(time_cycle_zeroed(fit_startpt),time_cycle_zeroed(fit_endpt),10
0000);

    fo = fitoptions('Method','NonlinearLeastSquares');
    ft = fittype(' a1*sin(b1*x+c1)','problem','b1','options',fo);
    [ch1.fit,ch1.G] = fit(X,Y,ft,'problem',fq*2*pi);
    fitted_ch1 = [fitted_ch1;abs(ch1.fit.a1)];                  % save
the amplitude of the fitted sine wave

end

%% polar plot

norm_fitted_ch1 = fitted_ch1./fitted_ch1(1);                    %
normalize about 0 degree
save(['fitted_',filename,'.mat'],'norm_fitted_ch1');
figure
theta = linspace(0,2*pi,num_step)';
polar(theta,fitted_ch1)
polar(theta,norm_fitted_ch1);
set(gca,'FontSize',14);
saveas(gcf,['d_',filename,'.fig']);
clc
% clear all
time_start
time_end

toc

% print(filename, '-dpng', '-r600'); %Save as PNG with 600 DP
```

Code for Extrapolation of Transfer function:

```
f=[500 1000 1500 2000 2500 3000 3500 3600 3800 4000 4500];
h=[1.5489 1.2744 0.3162 1.2859 1.120 0.1122 1.120 1.5849 1.5849 1.120
0.3981];
for k=1:11
ko=2*3.14*f(k)/340;
r=exp(-j*ko*0.077)-h(k)*exp(-
j*ko*(0.117+0.077))/(h(k)*exp(j*ko*(0.117+0.077)-exp(j*ko*0.077)));
zo(k)=(1+r)/(1-r)*(1100*340);
Zi(k)=imag(zo(k));
end
x=4000;
for count=1:6
g(count)=x+1000;
x=g(count);
end
```

```
for count=1:6
%Zinterp(count)=interp1(f,Zi,g(count),'cubic','extrap');
hinterp(count)=interp1(f,h,g(count),'cubic','extrap');
end
for k=1:6
ko=2*3.14*g(k)/340;
r=exp(-j*ko*0.077)-hinterp(k)*exp(-
j*ko*(0.117+0.077))/(hinterp(k)*exp(j*ko*(0.117+0.077)-
exp(j*ko*0.077)));
z(k)=(1+r)/(1-r)*(1100*340);
Zextrap(k)=imag(z(k));
end
FreqMat=horzcat(f,g);
H12Mat=horzcat(h,hinterp);
FreqMat2(1)=500;
x=500;
for count=2:51
FreqMat2(count)=x+190;
x=FreqMat2(count);
end
for count=1:51
%Zinterp(count)=interp1(f,Zi,g(count),'cubic','extrap');
HinterpGain(count)=interp1(FreqMat,H12Mat,FreqMat2(count),'cubic','extr
ap');
end
for k=1:51
ko=2*3.14*FreqMat2(k)/340;
r=exp(-j*ko*0.077)-HinterpGain(k)*exp(-
j*ko*(0.117+0.077))/(HinterpGain(k)*exp(j*ko*(0.117+0.077)-
exp(j*ko*0.077)));
z(k)=(1+r)/(1-r)*(1100*340);
end
% for count=1:51
% Index(count)=num2str(count);
% end
```